Nek2 phosphorylates and stabilizes β-catenin at mitotic centrosomes downstream of Plk1

Bertrade C. Mbom[a], Kathleen A. Siemers[a], Maggie A. Ostrowski[b], W. James Nelson[a,c], and Angela I. M. Barth[a]

[a]Department of Biology and [b]Department of Chemical Engineering, Stanford University, Stanford, CA 94305; [c]Department of Molecular and Cellular Physiology, Stanford University School of Medicine, Stanford, CA 94305

ABSTRACT **β-Catenin is a multifunctional protein with critical roles in cell–cell adhesion, Wnt signaling, and the centrosome cycle. Whereas the regulation of β-catenin in cell–cell adhesion and Wnt signaling are well understood, how β-catenin is regulated at the centrosome is not. NIMA-related protein kinase 2 (Nek2), which regulates centrosome disjunction/splitting, binds to and phosphorylates β-catenin. Using in vitro and cell-based assays, we show that Nek2 phosphorylates the same regulatory sites in the N-terminus of β-catenin as glycogen synthase kinase 3β (GSK3β), which are recognized by a specific phospho-S33/S37/T41 antibody, as well as additional sites. Nek2 binding to β-catenin appears to inhibit binding of the E3 ligase β-TrCP and prevents β-catenin ubiquitination and degradation. Thus β-catenin phosphorylated by Nek2 is stabilized and accumulates at centrosomes in mitosis. We further show that polo-like kinase 1 (Plk1) regulates Nek2 phosphorylation and stabilization of β-catenin. Taken together, these results identify a novel mechanism for regulating β-catenin stability that is independent of GSK3β and provide new insight into a pathway involving Plk1, Nek2, and β-catenin that regulates the centrosome cycle.**

Monitoring Editor
Monica Bettencourt-Dias
Instituto Gulbenkian de Ciência

Received: Jun 27, 2013
Revised: Jan 13, 2014
Accepted: Jan 27, 2014

INTRODUCTION

β-Catenin is a multifunctional protein that plays essential roles in cell–cell adhesion and Wnt signaling (Nelson and Nusse, 2004), as well as in bipolar spindle formation (Kaplan *et al.*, 2004). Phosphorylation of β-catenin by different kinases plays key roles in regulating the level, localization, and function of β-catenin in these different cellular processes.

β-Catenin plays an important role in the structural and functional organization of adherens junctions in cell–cell adhesion. β-Catenin binds tightly to the cytoplasmic domain of type I cadherins at the plasma membrane and to the actin-binding protein α-catenin (Weis and Nelson, 2006). The catenin–cadherin complex is regulated by serine/threonine phosphorylation of β-catenin (Bek and Kemler, 2002) and E-cadherin (Aberle *et al.*, 1994), which leads to stabilization of the cadherin–catenin complex. In abnormal or disease states, tyrosine phosphorylation of β-catenin disrupts the cadherin–catenin complex, causing reduction and/or loss of cell–cell adhesion and increase in cytoplasmic β-catenin (Roura *et al.*, 1999; Piedra *et al.*, 2003)

β-Catenin plays a key role in the canonical Wnt signaling pathway (Nelson and Nusse, 2004). Regulation of the level of cytoplasmic β-catenin is the central switch in the Wnt pathway. In the absence of Wnt, cytoplasmic levels of β-catenin are low due to degradation by the destruction complex. The destruction complex consists of the scaffold proteins adenomatous polyposis coli (APC) and axin, which bind β-catenin and glycogen synthase kinase 3β (GSK3β). GSK3β and its priming kinase, casein kinase 1 (CK1), phosphorylate β-catenin at residues S33/S37/T41 and S45, respectively, leading to binding of the E3 ligase β-TrCP, which marks β-catenin for ubiquitination and then degradation by the proteasome (Hart *et al.*, 1999). Conversely, Wnt binding to the transmembrane receptor frizzled inhibits β-catenin phosphorylation by the destruction complex, causing β-catenin to accumulate in the cytoplasm. This stable pool of β-catenin is translocated to the nucleus and binds to the

This article was published online ahead of print in MBoC in Press (http://www.molbiolcell.org/cgi/doi/10.1091/mbc.E13-06-0349) on February 5, 2014.

Address correspondence to: Angela Barth (angelab@stanford.edu).

Abbreviations used: APC, adenomatous polyposis coli; β-catenin*, alanine substitutions of GSK3β/CK1 phosphorylation sites (S33/S37/T41 and S45) in β-catenin; CK1, casein kinase 1; GSK3β, glycogen synthase kinase 3β; KD Nek2, kinase-dead Nek2; Nek2, NIMA-related kinase 2; Plk1, polo-like kinase 1; Tcf/Lef, T-cell factor/lymphoid enhanced factor.

T-cell factor/lymphoid enhanced factor (Tcf/Lef) to induce transcription of specific target genes (Morin *et al.*, 1997; Arias *et al.*, 1999; Huelsken and Behrens, 2002; Logan and Nusse, 2004).

In addition to these roles in Wnt signaling and cell–cell contact, β-catenin is a component of the centrosome (Kaplan *et al.*, 2004). In mammalian cells, the centrosome is the major organizer of the microtubule cytoskeleton (Azimzadeh and Bornens, 2007). During interphase, the centrosome coordinates an astral array of microtubules that participate in intracellular trafficking, cell motility, cell adhesion, and cell polarity (Azimzadeh and Bornens, 2007). β-Catenin localizes to centrosomes in interphase and mitosis and functions to ensure proper centrosome disjunction and bipolar spindle formation (Kaplan *et al.*, 2004; Bahmanyar *et al.*, 2008). Depletion of β-catenin leads to an increase in monopolar spindles (Kaplan *et al.*, 2004), which consist of centrosomes in close proximity surrounded by the chromosomes. These data identified a novel role for β-catenin in promoting centrosome disjunction (Kaplan *et al.*, 2004). A stabilized form of β-catenin, with alanine substitutions of GSK3β/CK1 phosphorylation sites (S33/S37/T41 and S45; β-catenin*), also localizes to centrosomes and has a decreased turnover compared with wild-type β-catenin at centrosomes in interphase cells (Bahmanyar *et al.*, 2008, 2010). Stabilization of β-catenin results in premature centrosome disjunction (Bahmanyar *et al.*, 2008) and the formation of extra non-microtubule-nucleating structures (Kuriyama *et al.*, 2009; Bahmanyar *et al.*, 2010). Neuronal progenitor cells in mice that express only this phospho-mutant β-catenin have defects in microtubule organization and cell polarity, similar to the phenotype in β-catenin loss-of-function neuronal progenitor cells (Chilov *et al.*, 2011). Decreased centrosomal levels of phospho-S33/S37/T41 β-catenin are associated with reduced γ-tubulin at centrosomes and reduced microtubules (Chilov *et al.*, 2011). Taken together, these results indicate that β-catenin stability may be sufficient for some functions (e.g., centrosome disjunction), and phospho sites may be required for others (e.g., microtubule organization).

It has been concluded that GSK3β phosphorylates S33/S37/T41 sites on β-catenin at centrosomes, resulting in the stabilization of β-catenin at centrosomes (Hadjihannas *et al.*, 2010; Chilov *et al.*, 2011), even though this is the opposite effect of the well-characterized role of GSK3β phosphorylation in destabilizing β-catenin by targeting it for degradation (Hart *et al.*, 1999). These conclusions on the role of GSK3β in regulating centrosomal β-catenin have been based on immunofluorescence studies with the antibody that recognizes the phospho-S33/S37/T41 peptide.

In addition to GSK3β, the NIMA-related kinase 2 (Nek2) binds to and phosphorylates β-catenin (Bahmanyar *et al.*, 2008). Structurally, the Nek family of proteins contains an N-terminal catalytic kinase domain and a C-terminal regulatory domain. Nek kinases play important roles in cell cycle progression, ciliogenesis, and microtubule organization (Quarmby and Mahjoub, 2005). Nek2 is a core component of the centrosome throughout the cell cycle, but its kinase activity is regulated during the cell cycle and peaks in mitosis (Fry, 2002). Nek2 localizes to nucleoli during interphase (White and Quarmby, 2008), on condensed chromatin in mitotic and meiotic cells (Fujioka *et al.*, 2000; Ha Kim *et al.*, 2002), at kinetochores (Merle *et al.*, 2005), and at the midbody of dividing cells (Ha Kim *et al.*, 2002). Nek2 kinase activity is regulated by polo-like kinase 1 (Plk1), an important mitotic kinase that regulates centrosome maturation, including the recruitment of γ-tubulin and other centrosome components at G2/M (Mardin *et al.*, 2011; Wang *et al.*, 2013). Nek2 is required for centrosome disjunction and bipolar spindle formation (Faragher and Fry, 2003). A kinase-dead form of Nek2 (KD Nek2) causes formation of monopolar spindles and abnormal spindle formation and chromosome segregation (Faragher and Fry, 2003).

Similar to Nek2, β-catenin localizes to centrosomes throughout the cell cycle, and β-catenin localization to interphase centrosomes is mediated by the linker proteins rootletin and C-Nap1 (Bahmanyar *et al.*, 2008). Nek2 activity is regulated during the cell cycle and peaks at the G2/M boundary (Fry, 2002) when β-catenin localization to centrosomes becomes independent of rootletin and C-Nap1 (Bahmanyar *et al.*, 2008). The centrosome linker proteins rootletin and C-Nap1 are phosphorylated by Nek2 and, as a consequence, are removed from centrosomes, resulting in centrosome disjunction (Fry *et al.*, 1998; Bahe *et al.*, 2005; Bahmanyar *et al.*, 2008). Thus the peak of Nek2 activity at the G2/M boundary (Fry, 2002) coincides with a linker-protein independent increase of β-catenin at centrosomes (Bahmanyar *et al.*, 2008).

Given the proposed role for phospho–β-catenin in centrosomes cohesion, we sought to dissect how this specific pool of β-catenin was regulated. Using in vitro and cell-based assays, we show that Nek2 directly phosphorylates β-catenin at S33/S37/T41 and additional sites. Of interest, Nek2 blocks β-catenin interaction with β-TrCP, thereby inhibiting β-catenin ubiquitination and degradation and resulting in the accumulation of Nek2-phosphorylated β-catenin at centrosomes. Finally, we show that Nek2, not GSK3β, regulates phospho-S33/S37/T41 reactivity and β-catenin at spindle poles downstream of Plk1.

RESULTS

Nek2 directly phosphorylates β-catenin at known GSK3β sites (S33/S37/T41) and additional amino acids

β-Catenin was shown to be a substrate for Nek2 (Bahmanyar *et al.*, 2008). To identify the amino acids in β-catenin phosphorylated by Nek2, we performed liquid chromatography–tandem mass spectrometry (LC-MS/MS) on purified β-catenin that had been expressed and purified from bacteria and then phosphorylated in vitro with purified Nek2 in the presence of ATP. As a control, we analyzed a sample of β-catenin incubated with Nek2 in the absence of ATP. The Nek2 phosphorylation sites identified in β-catenin were S23, S29, S33, T102, T556, S675, and amino acids within S37–T42 (Figure 1A; LC-MS/MS results in | Supplemental Figure S1 and Supplemental Table S1); note that the GSK3β phosphorylation sites are S33, S37, and T41.

To test whether Nek2 directly phosphorylated S33/S37/T41 of β-catenin, we used an antibody specific for the phospho-S33/S37/T41 peptide. We performed in vitro phosphorylation assays with glutathione *S*-transferase (GST)–tagged β-catenin N-terminal domain (amino acids 1–133) and histidine (His)-tagged Nek2; as a positive control, N-terminal β-catenin was also incubated with GSK3β and CK1 (Figure 1, B and C). Western blotting showed a strong signal for phospho-S33/S37/T41 β-catenin in the presence of either Nek2 (Figure 1C, lane 4, asterisk) or GSK3β/CK1 (Figure 1C, lane 2, asterisk). Note that β-catenin phosphorylated by Nek2 (Figure 1, B and C, lane 4) migrated more slowly in SDS–PAGE than β-catenin phosphorylated by GSK3β/CK1 (Figure 1, B and C, lane 2), which is likely due to the additional Nek2 phosphorylation sites in the β-catenin N-terminus (Figure 1A and Supplemental Figure S1). These results show that Nek2, like GSK3β, directly phosphorylated sites in the N-terminus of β-catenin that are recognized by the phospho-S33/S37/T41 antibody. Although we could not definitively identify the Nek2 phosphorylation site(s) in the region of S37–T42 of β-catenin, recognition of Nek2-phosphorylated β-catenin by an antibody made against a synthetic phospho-S33/S37/T41 peptide of this region indicates that Nek2

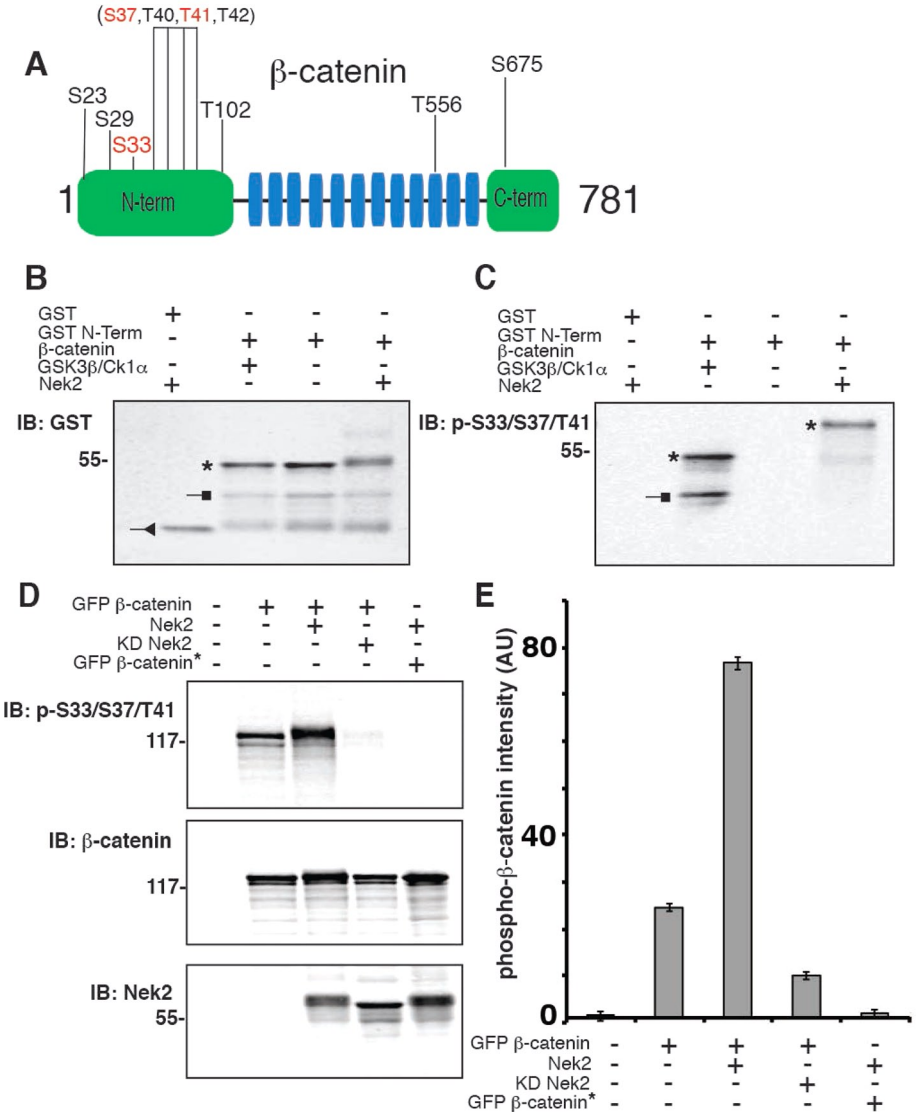

FIGURE 1: Nek2 phosphorylates β-catenin at known GSK3β S33/S37/T41 sites and additional residues. (A) Schematic representation of β-catenin, with the armadillo repeats highlighted in blue (not to scale). The phosphorylated amino acids identified by nano-LC/MS/MS are shown only for the sample incubated with ATP. As a control, an identical sample without ATP was also analyzed. Known GSK3β phosphorylation sites are highlighted in red. The bracketed residues indicate a region of the peptide in which specific phospho site(s) could not be distinguished. (B, C) In vitro phosphorylation assay of GST protein and GST-N-terminal β-catenin (amino acids 1–133) purified from bacteria and incubated with recombinant kinases as indicated for 60 min in the presence of ATP, separated by SDS–PAGE, and Western blotted with an antibody to GST (B) or an antibody to the phospho-S33/S37/T41 epitope (C); phosphorylated β-catenin is marked by an asterisk, degradation products by a square, and GST by a triangle. (D) HEK293 cells cotransfected as indicated and treated for 4 h with GSK3 inhibitor (20 μM SB21673), extracted with 1% SDS, and immunoblotted with antibodies to detect phospho-S33/S37/T41 β-catenin and Nek2. (E) Quantitation of phospho–β-catenin band intensity normalized for total GFP–β-catenin (AU, arbitrary units); error bars, SEM of three independent experiments.

phospho sites comprise the same sites that are phosphorylated by GSK3β.

We used a cell-based assay to test whether Nek2 phosphorylated S33/S37/T41 sites in β-catenin in whole cells. HEK293 cells were transiently cotransfected with green fluorescent protein (GFP)–tagged β-catenin and with Nek2 or KD Nek2. Cells were treated with the GSK3β inhibitor SB216763 and the CK1α inhibitor D4476 (MacLaine *et al.*, 2008) to distinguish Nek2-specific phosphorylation of β-catenin. Cell lysates were Western blotted with antibodies specific for phospho-S33/S37/T41, β-catenin, and Nek2 (Figure 1D).

Some phospho-S33/S37/T41 β-catenin was detected in lysates from cells transfected with GFP–β-catenin and treated with GSK3β and CK1α inhibitors (Figure 1, D and E); this might be due to residual activity of endogenous GSK3β and CK1α or another endogenous kinase such as Nek2 (note that inhibitors specific for Nek2 are not available). Significantly, coexpression of Nek2 and GFP–β-catenin resulted in a threefold increase in the level of phospho-S33/S37/T41 β-catenin (detected by Western blotting with the phospho-S33/S37/T41 antibody) compared with its level in cells in the absence of exogenous Nek2 (Figure 1, D and E). In contrast, coexpression of KD Nek2 resulted in a significant reduction in the level of phospho-S33/S37/T41 β-catenin compared with its levels in the absence or presence of exogenous Nek2 (Figure 1, D and E). We hypothesize that the reduction in the background signal of phospho–β-catenin in the presence of KD Nek2 occurs because KD Nek2 binds to β-catenin and thereby competes with endogenous kinases, reducing phosphorylation at that site. The expression of neither Nek2 nor KD Nek2 affected the level of GFP–β-catenin in cells (Figure 1D).

As a negative control, Nek2 was coexpressed with GFP-β-catenin* containing alanine substitutions of S33, S37, T41, and S45; this mutant cannot be phosphorylated by GSK3β/CK1α at these sites and is insensitive to degradation by the proteasome (Barth *et al.*, 1999). Western blotting showed that the level of phospho-S33/S37/T41 in GFP-β-catenin* (Figure 1, D and E, lane 5) was close to the background in nontransfected cells (Figure 1, D and E, lane 1), indicating that there is no detectable phosphorylation of β-catenin* at those sites and confirming that this antibody is specific for phospho-S33/S37/T41 in Nek2-phosphorylated β-catenin.

Taken together, the results of these in vitro and cell-based assays demonstrate that Nek2 phosphorylates β-catenin at S33/S37/T41 and at least five additional sites. Furthermore, phosphorylation of the S33/S37/T41 sites by Nek2 is independent of GSK3β and CK1α activities.

Nek2 phosphorylation results in β-catenin stabilization

It is well known that GSK3β phosphorylation of β-catenin at S33/S37/T41 targets β-catenin for ubiquitination by the E3 ligase, β-TrCP, and subsequent degradation by the proteasome (Hart *et al.*, 1999). To test whether Nek2 phosphorylation of β-catenin

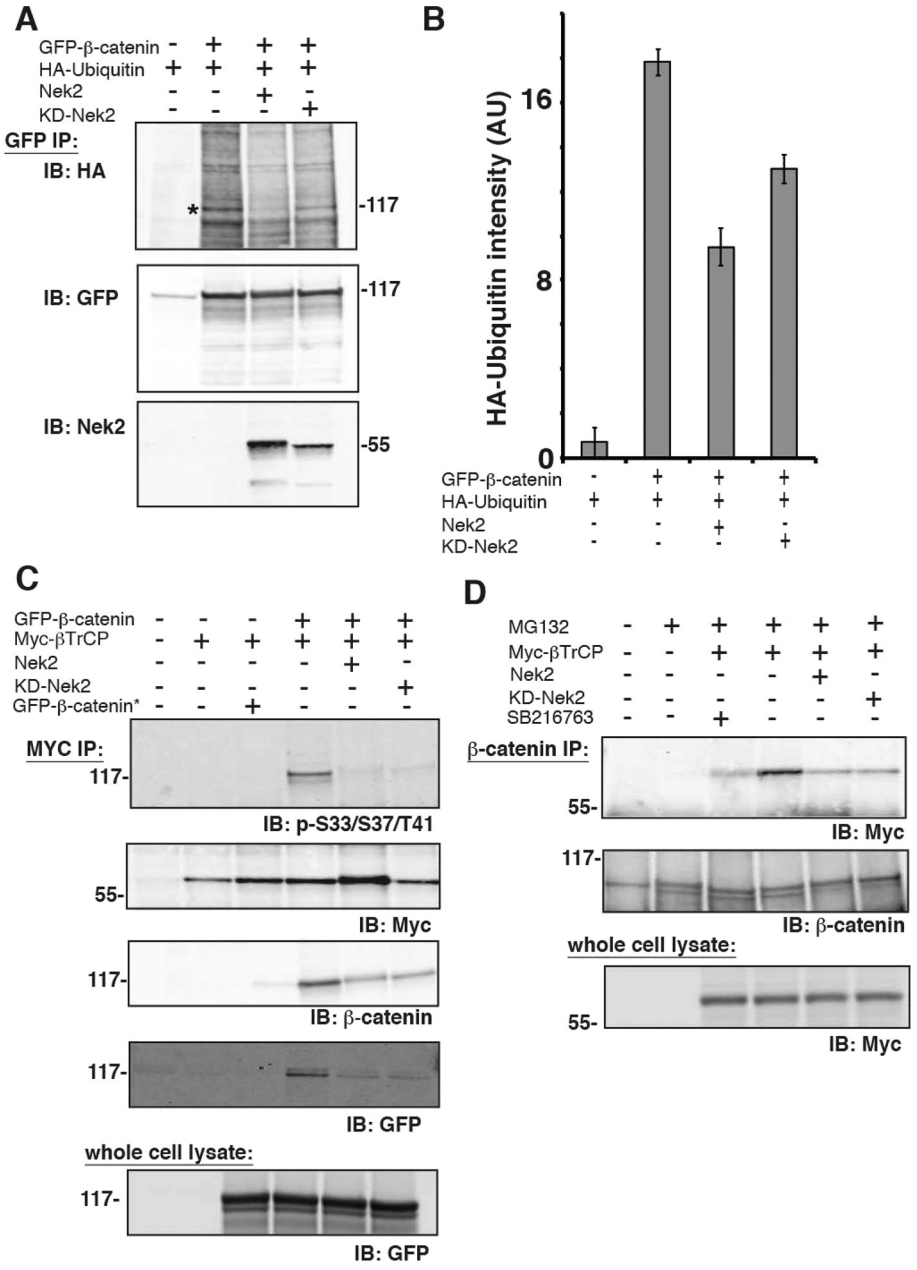

FIGURE 2: Nek2 stabilizes β-catenin. (A) HEK293 cells were cotransfected as indicated and extracted with NP40, and proteins were immunoprecipitated with polyclonal GFP antibody and immunoblotted with a monoclonal antibody to HA, a polyclonal antibody to GFP, or a monoclonal antibody to Nek2. (B) Quantitation of HA-ubiquitin band intensity (AU, arbitrary units); error bars, SEM of three independent experiments. (C) HEK293 cells were cotransfected as indicated and extracted with NP40, and proteins were immunoprecipitated with a Myc antibody and immunoblotted with antibodies specific for phospho-S33/S37/T41, β-catenin, GFP, and Myc. Whole-cell lysates were immunoblotted for GFP. (D) HEK293 cells cotransfected as indicated and treated for 4 h with proteasome inhibitor (25 μM MG132) and GSK3 inhibitor (20 μM SB21673) as indicated. Cell lysates were extracted with NP40, immunoprecipitated with a β-catenin antibody, and then immunoblotted for β-catenin and Myc. Whole-cell lysates were immunoblotted for Myc.

at those sites affected levels of ubiquitinated β-catenin, we cotransfected HEK293 cells with GFP–β-catenin, hemagglutinin (HA)-ubiquitin and either Nek2 or KD Nek2. GFP–β-catenin was immunoprecipitated with a GFP antibody, separated by SDS–PAGE, and Western blotted with HA- and GFP-specific antibodies (Figure 2A).

GFP immunoprecipitation of lysates from cells expressing GFP–β-catenin resulted in the coimmunoprecipitation of β-catenin and bound HA-ubiquitin (Figure 2, A, lane 2, and B); HA-ubiquitin was not immunoprecipitated with the GFP antibody in the absence of GFP–β-catenin (Figure 2, A, lane 1, and B). Expression of Nek2 or KD Nek2 resulted in 50 and 33% decrease, respectively, in level of HA-ubiquitin–bound β-catenin compared with control (Figure A, lanes 3 and 4 vs. lane 2, and B). Ubiquitination of β-catenin was confirmed by treating immunoprecipitates with the deubiquitinating enzyme Usp2 before protein separation by SDS–PAGE, which resulted in significantly reduced levels of HA-ubiquitin bound to β-catenin (Supplemental Figure S2).

Western blotting of GFP–β-catenin immunoprecipitates with a Nek2 antibody revealed that Nek2 and KD Nek2 coimmunoprecipitated with GFP–β-catenin (Figure 2A, Nek2 blot). Thus the interaction of Nek2 and β-catenin does not require Nek2 activity, occurs in the absence of β-catenin phosphorylation, and decreases the level of ubiquitinated β-catenin. This last is opposite to the effect of phosphorylation of β-catenin by GSK3β, which results in increased levels of ubiquitinated β-catenin (Liu *et al.*, 2002).

β-Catenin is ubiquitinated by binding the E3 ligase β-TrCP (Hart *et al.*, 1999). Therefore we tested whether the lack of ubiquitination of β-catenin in the presence of Nek2 reflected a block in β-TrCP binding to β-catenin. HEK293 cells were cotransfected with either GFP–β-catenin* or GFP–β-catenin and Myc–β-TrCP. Myc–β-TrCP was immunoprecipitated with a Myc antibody, and immunoprecipitates were Western blotted for phospho-S33/S37/T41, Myc, β-catenin, and GFP (Figure 2C). GFP–β-catenin* was not coimmunoprecipitated with Myc–β-TrCP (Figure 2C, lane 3), as expected due to the absence of phospho-S33/S37/T41 sites. However, GFP–β-catenin, which contains the phospho-S33/S37/T41 sites, was coimmunoprecipitated with Myc–β-TrCP (Figure 2C, lane 4). In the presence of Nek2 or KD Nek2, however, levels of total GFP–β-catenin and phospho-S33/S37/T41 β-catenin decreased by 53% in Myc–β-TrCP immunoprecipitates (Figure 2C, compare lanes 5 and 6 to lane 4).

To test whether β-TrCP binding to endogenous β-catenin was affected by expressing Nek2, we cotransfected HEK293 cells with Myc–β-TrCP and either Nek2 or KD Nek2 and then treated them with MG132 to inhibit the proteasome. β-Catenin immunoprecipitates were Western blotted with Myc or β-catenin antibodies (Figure 2D). The level of β-TrCP coimmunoprecipitated with β-catenin was highest in the presence of MG132 (Figure 2D, lane 4). Addition of the GSK3β

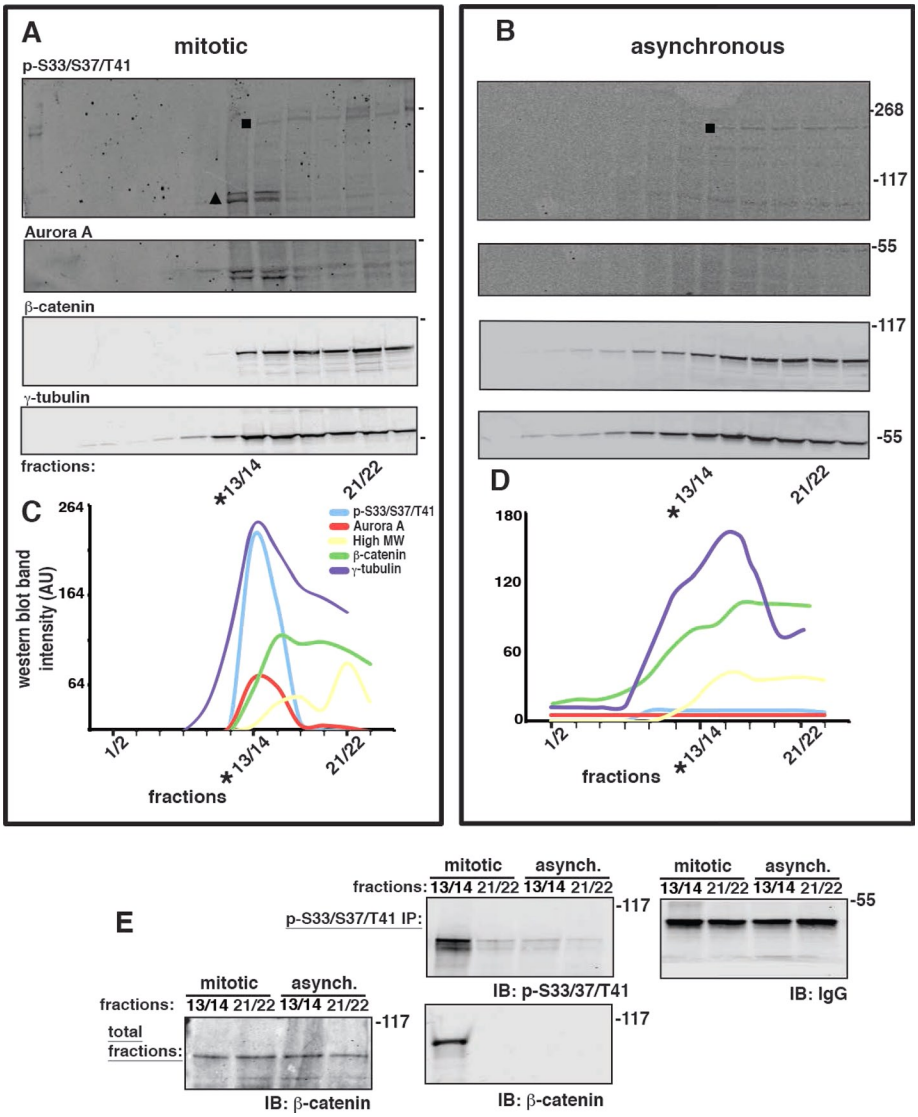

FIGURE 3: Phospho–β-catenin is located at mitotic centrosomes. (A) HCT116 $18^{-/\Delta S45}$ cells were synchronized in mitosis. Centrosomes were enriched in a sucrose gradient, and fractions were immunoblotted for phospho-S33/S37/T41, Aurora A, β-catenin, and γ-tubulin. (B) Centrosomes from an asynchronous population of HCT116 $18^{-/\Delta S45}$ cells were enriched and immunoblotted as described in A. (C, D) Indicated protein bands from blots in A and B were quantified (square in top blots indicate HMW protein(s), and triangle in top mitotic blot indicates phospho-S33/S37/T41 β-catenin; double bands of phospho-S33/S37/T41 β-catenin and Aurora A were combined for quantitation). Distributions are presented on the same graph, but levels (AU) of proteins are not comparable, as different antibodies were used for each protein. (E) Centrosome-positive fractions (*13/14) and centrosome-negative fractions (21/22) from mitotic and asynchronous centrosome preparations, respectively, were immunoprecipitated with phospho-S33/S37/T41 antibody (p-S33/S37/T41 IP) and immunoblotted (IB) with antibodies to phospho-S33/37/T41 (p-S33/S37/T41) and β-catenin. Levels of immunoglobulin heavy chain (IgG) in the immunoprecipitations are shown as a control (IB: IgG in E). Part of the original fractions of the sucrose gradients shown in A and B that were used for immunoprecipitations were combined into one immunoblot for comparison of total β-catenin levels in these fractions (total fractions in E, immunoblotted for β-catenin).

inhibitor SB21673 decreased binding of β-TrCP to endogenous β-catenin (Figure 2D, compare lane 3 to lane 4), as expected, since β-TrCP specifically binds to GSK3β-phosphorylated S33/S37/T41 sites on β-catenin (Orford *et al.*, 1997; Wu *et al.*, 2003). In the presence of Nek2 or KD Nek2, β-TrCP binding to endogenous β-catenin was reduced to background levels (Figure 2D, compare lanes 5 and 6 to lanes 3 and 4).

Taken together, these results show that β-TrCP binding to β-catenin is reduced in the presence of either Nek2 or KD Nek2. These results indicate that Nek2 competes with β-TrCP for binding to β-catenin independent of Nek2 activity, although additional experiments are needed to test this mechanism directly.

Phospho–β-catenin is located at mitotic centrosomes

Because the interaction of Nek2 and β-catenin was originally identified at centrosomes (Bahmanyar *et al.*, 2008), it was important to determine whether phosphorylation of S33/S37/T41 on β-catenin occurred at centrosomes. Previous immunofluorescence studies with the phospho-S33/S37/T41 antibody were interpreted as evidence that the level of centrosomal phospho-S33/S37/T41 β-catenin was GSK3β dependent and increased at the onset of mitosis (Huang *et al.*, 2007; Hadjihannas *et al.*, 2010).

To test directly whether GSK3β caused S33/S37/T41 β-catenin phosphorylation at centrosomes during mitosis, we used variants of the HCT116 cell line in which the wild-type β-catenin allele had been deleted and the other β-catenin allele contained an in-frame deletion of serine 45 ($18^{-/\Delta S45}$) (Kim *et al.*, 2002a); ΔS45 inhibits GSK3β-specific phosphorylation of S33/S37/T41 on β-catenin because the CK1α priming phosphorylation on S45 is deleted (Supplemental Figure S4; Liu *et al.*, 2002). Cells were collected from either an asynchronous population or a population synchronized for collection in mitosis, and centrosomes were enriched in a sucrose gradient (Bornens *et al.*, 1987; Supplemental Figure S3, A and B). All gradient fractions from mitotic and asynchronous populations were analyzed by Western blotting for known centrosome marker proteins (Figure 3A). Phospho-S33/S37/T41 β-catenin from mitotic cells (Figure 3A, triangle) was enriched in fractions 13/14 (*13/14 in Figure 3A), which contained peaks in the distributions of γ-tubulin and the mitotic centrosome marker Aurora A (Figure 3, A and C). Double bands were sometimes observed for phospho-S33/S37/T41 β-catenin and Aurora A (Figure 3A, triangle) that might be due to phosphorylation or partial degradation. In addition to β-catenin, the phospho-S33/S37/T41 antibody also recognized a high–molecular weight (HMW) protein in some fractions (Figure 3, A and B, square). However, this HMW protein did not appear to cofractionate with phospho-S33/S37/T41 β-catenin or the centrosome marker proteins (*13/14 in Figure 3, A and C). Centrosome-enriched fractions from asynchronous cells (*13/14 in Figure 3B)

contained β-catenin and γ-tubulin but neither phospho-S33/S37/T41 β-catenin nor Aurora A (Figure 3, B and D), demonstrating that the presence of phospho-S33/S37/T41 β-catenin was specific for mitotic centrosomes.

To confirm the identity of phospho-β-catenin in mitotic centrosome fractions, we immunoprecipitated phospho-S33/S37/T41-reactive protein(s) from centrosome-enriched peak fractions (*13/14; defined by the peak of γ-tubulin in the gradient) and fractions that were not enriched for centrosomes (21/22) from mitotic and asynchronous cells, respectively. The immunoprecipitates were Western blotted with antibodies for β-catenin and phospho-S33/S37/T41 (Figure 3E), and the original fractions (i.e., before immunoprecipitation) were also blotted for β-catenin to verify that total levels of β-catenin were equivalent. Phospho-S33/S37/T41 β-catenin was immunoprecipitated from mitotic centrosome-enriched fractions (Figure 3E); a weak signal of a phospho-S33/S37/T41–reactive HMW protein was also detected when the Western blot was overexposed (Supplemental Figure S3C). Very little phospho-S33/S37/T41 β-catenin was detected in phospho-S33/S37/T41 antibody immunoprecipitates from centrosome-enriched fractions prepared from asynchronous cells (Figure 3E).

These results indicate that phospho-S33/S37/T41 β-catenin is present in centrosomes during mitosis. Because we used a cell line, HCT116 $18^{-/\Delta S45}$, expressing only ΔS45 β-catenin for the centrosome preparations, we conclude that phosphorylation of S33/S37/T41 β-catenin at mitotic centrosomes is not caused by GSK3β activity (see also Figure 4 and Supplemental Figure S4).

Deletion of the CK1 phosphorylation-priming site (ΔS45) for GSK3β phosphorylation in β-catenin does not affect the majority of phospho-S33/S37/T41 reactivity at spindle poles

Phospho-S33/S37/T41 reactivity at spindle pole bodies was observed by immunofluorescence in previous studies (Huang *et al.*, 2007; Hadjihannas *et al.*, 2010; Chilov *et al.*, 2011). Using HCT116 cells with different combinations of wild-type and mutant β-catenin alleles, we could test directly whether CK1 priming of the S45 residue is required for phospho-S33/S37/T41 reactivity at spindle poles. We used the following three cell lines: 1) parental HCT116 cells containing a wild-type β-catenin allele and a β-catenin mutant allele with an in-frame deletion of serine 45 ($Par^{WT/\Delta S45}$); 2) HCT116 cells containing the mutant β-catenin allele and a deletion of the wild-type β-catenin allele ($18^{-/\Delta S45}$); and 3) HCT116 cells containing a wild-type β-catenin allele and a deletion of the mutant β-catenin allele ($85^{WT/-}$; Kim *et al.*, 2002a). Compared to the parental line $Par^{WT/\Delta S45}$, total levels of β-catenin were lower (30–40%) in $85^{WT/-}$ with only wild-type β-catenin and approximately the same in $18^{-/\Delta S45}$ with only stabilized β-catenin (Supplemental Figure S4; Bahmanyar *et al.*, 2010).

To determine the total amount of phospho-S33/S37/T41 reactivity at spindle pole bodies, we measured the mean fluorescence intensity at spindle poles in mitotic cells stained with the phospho-S33/S37/T41 antibody, the microtubule marker α-tubulin, and the centrosome marker γ-tubulin. Phospho-S33/S37/T41 reactivity colocalized with γ-tubulin–labeled centrosomes in mitotic cells in all three HCT116 cells lines, including $18^{-/\Delta S45}$ cells, which were completely deficient of the CK1-priming site for GSK3β phosphorylation on β-catenin (Figure 4A). Phospho-S33/S37/T41 reactivity was increased at spindle poles in cells that have wild-type β-catenin compared with $18^{-/\Delta S45}$ cells (Figure 4B: $Par^{WT/\Delta S45}$ 21% higher than $18^{-/\Delta S45}$, $^{**}p < 0.01$; $85^{WT/-}$ 34% higher than $18^{-/\Delta S45}$, $^{***}p < 0.001$); this could be regulated by GSK3β activity (Hadjihannas *et al.*, 2010). The total level of β-catenin was decreased at spindle poles of $85^{WT/-}$ cells compared with $18^{-/\Delta S45}$ cells (45% lower than $18^{-/\Delta S45}$, $^{***}p < 0.001$; Figure 4C), consistent with our previous result (Bahmanyar *et al.*, 2010) that phospho-mutant β-catenin* is stabilized at centrosomes.

To test whether the majority of phospho-S33/S37/T41 reactivity at spindle poles is independent of GSK3β, we used three different inhibitors of GSK3β and measured the fluorescence intensity of phopsho-S33/S37/T41 reactivity at mitotic spindle poles in the HCT116 lines (Figure 4D for parental HCT116 cells $Par^{WT/\Delta S45}$; Supplemental Figure S4, B and C, for $18^{-/\Delta S45}$ and $85^{WT/-}$ cells; and Figure 4E). The activity of these inhibitors was confirmed by showing overall reduction in MG132-stabilized phospho-S33/S37/T41 β-catenin levels in whole-cell SDS extracts from asynchronous HCT116 $Par^{WT/\Delta S45}$ populations (Supplemental Figure S4). Significantly, we did not detect a statistically significant difference in fluorescence intensity levels of phospho-S33/S37/T41 reactivity at spindle poles in HCT116 $Par^{WT/\Delta S45}$, $18^{-/\Delta S45}$, or $85^{WT/-}$ cells that were treated with 0.2% dimethyl sulfoxide (DMSO), 20 μM SB21673 (Thotala *et al.*, 2008), or 5 μM 6-bromoindirubin-3′ oxime (GSK3 inhibitor IX; Meijer *et al.*, 2003; Figure 4D and Supplemental Figure S4, B and C). Only $Par^{WT/\Delta S45}$ and $85^{WT/-}$ cells treated with 20 mM LiCl had a small (~20%) reduction in fluorescence intensity of phospho-S33/S37/T41 reactivity at mitotic spindle poles (Figure 4E), which could be caused by inhibition of GSK3β phosphorylation of wild-type β-catenin in these cells (Hadjihannas *et al.*, 2010).

As expected, mitotic spindle poles in $18^{-/\Delta S45}$ cells had no reduction of phospho-S33/S37/T41 reactivity in the presence of all three GSK3β inhibitors (Figure 4E) and also showed no overall GSK3β-dependent accumulation of phospho-S33/S37/T41 β-catenin after MG132 treatment (Supplemental Figure S4; Liu *et al.*, 2002). Because $18^{-/\Delta S45}$ cells expressed phospho-S33/S37/T41 β-catenin at mitotic centrosomes (Figure 3), we conclude that phosphorylation of these sites in β-catenin is predominantly GSK3β independent at mitotic centrosomes.

Nek2 activity is required for phospho-S33/S37/T41 reactivity at spindle poles

We showed that Nek2 phosphorylates within the S33/37/T41 residues of β-catenin (Figure 1) and that the phospho-pool of β-catenin at mitotic centrosomes (Figure 3) is not regulated by GSK3β (Figure 4). Therefore we sought to determine whether Nek2 activity directly affected levels of phospho-S33/S37/T41 reactivity at mitotic spindle poles. U2OS cells transiently expressing HA-KD Nek2 or HA-WT-Nek2 were synchronized at the onset of mitosis. KD Nek2 caused the formation of monopolar spindles (Figure 5, A and C), as described previously (Faragher and Fry, 2003). We immunostained cells for β-catenin and the centrosomal marker γ-tubulin and then measured the mean fluorescence intensity of β-catenin at spindle poles of bipolar metaphase spindles or monopolar spindles induced by KD Nek2 (Figure 5, A and B). Compared to control levels, total β-catenin levels at spindle poles were not affected in monopolar spindles formed in the presence of KD Nek2 (Figure 5, A and B).

Spindle poles of monopolar spindles induced by overexpression of KD Nek2 had a statistically significant decrease (~60%) in mean fluorescence intensity of phospho-S33/S37/T41 reactivity compared with control bipolar spindle poles (Figure 5, C and D). Note that the level of phospho-S33/S37/T41 reactivity was likely reduced even more than that measured because the individual spindle poles could not be resolved and measured separately in most of these monopolar spindles.

In contrast, transfection with HA-WT-Nek2 did not affect the levels of phospho-S33/S37/T41 reactivity at the poles of bipolar

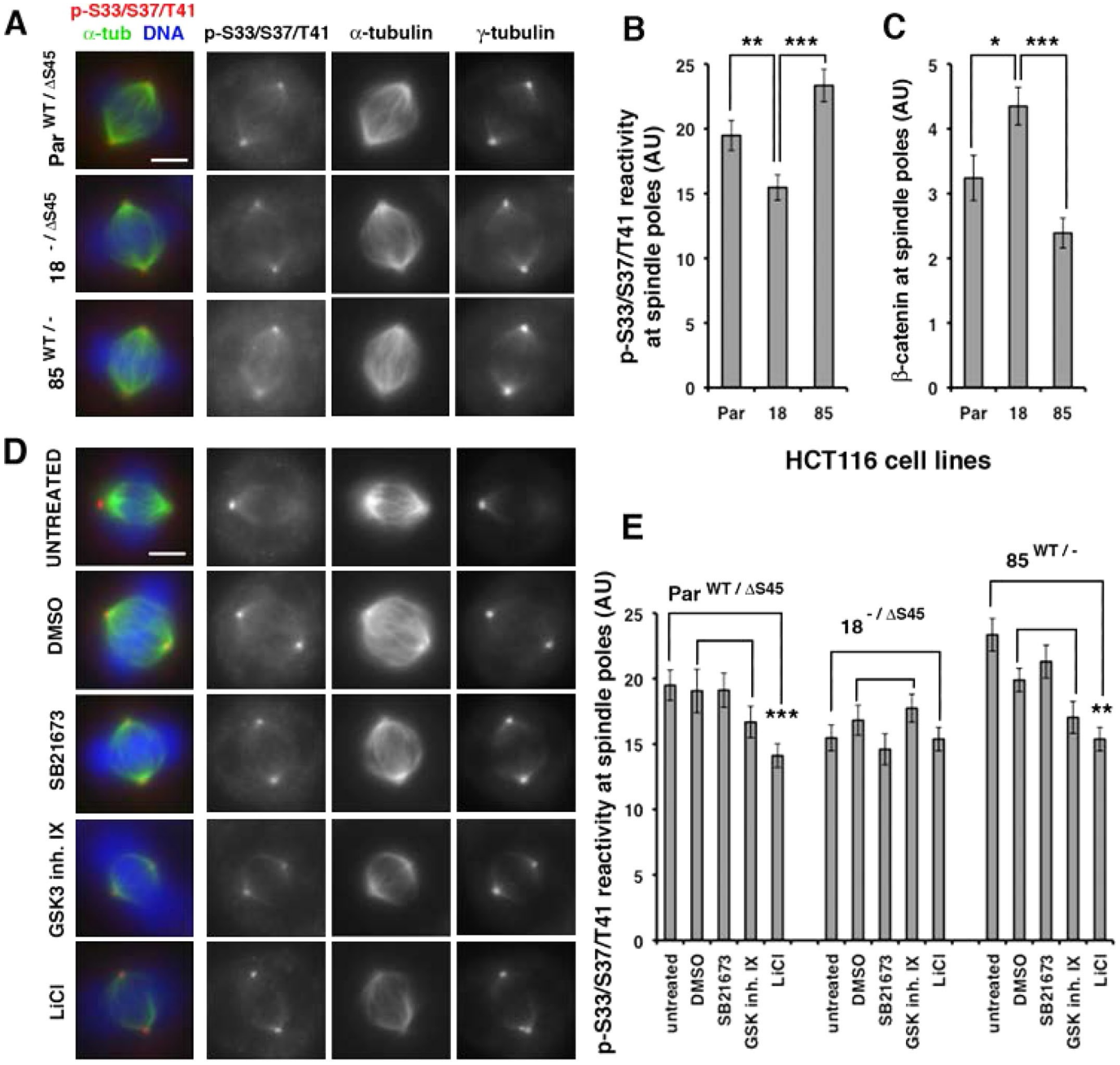

FIGURE 4: GSK3β activity is not required for phospho-S33/S37/T41 reactivity at spindle poles. (A) Spindles derived from three HCT116 lines expressing wild-type β-catenin and ΔS45 β-catenin ($Par^{WT/\Delta S45}$), only ΔS45 β-catenin ($18^{-/\Delta S45}$), or only wild-type β-catenin ($85^{WT/-}$) were stained for DNA with DAPI and immunostained with antibodies as indicated. Images were taken at identical exposure times and identically contrast enhanced for each stain. Scale bar, 5 μm. (B) Quantitation of phospho-S33/S37/T41 reactivity and (C) total β-catenin levels at spindle poles of cell lines in A. Error bars, SEM of ≥20 spindle poles; ***$p < 0.001$; **$p < 0.01$; *$p < 0.05$. Original unmodified images taken at identical exposure times were measured for the three cell lines (AU, arbitrary units). HCT116 $18^{-/\Delta S45}$ cells had significantly more β-catenin but less phospho-S33/S37/T41 reactivity at spindle poles than parental $Par^{WT/\Delta S45}$ and $85^{WT/-}$ cells (*$p < 0.05$; **$p < 0.01$; ***$p < 0.001$). (D) HCT116 $Par^{WT/\Delta S45}$ cells were treated with 2% DMSO as a control or with different GSK3 inhibitors (20 μM SB21673, 5 μM GSK3 Inhibitor IX, or 20 mM LiCl) for 4 h and then processed for immunofluorescence of mitotic spindles with antibodies as indicated and costained with DAPI for DNA (blue in merge). For presentation of control spindles and different treatments, images were taken at identical exposure times and identically contrast enhanced for each stain. Scale bar, 5 μm. (E) Phospho-S33/S37/T41 reactivity at spindle poles in different HCT116 lines described in A, untreated (same as in graph 4B), or treated as described in D (AU, arbitrary units). Error bars, SEM of ≥18 spindle poles; ***$p < 0.001$ and **$p < 0.01$. Original unmodified images taken at identical exposure times were measured for controls and different treatments. The data are representative of two independent experiments done with all cell lines under identical conditions.

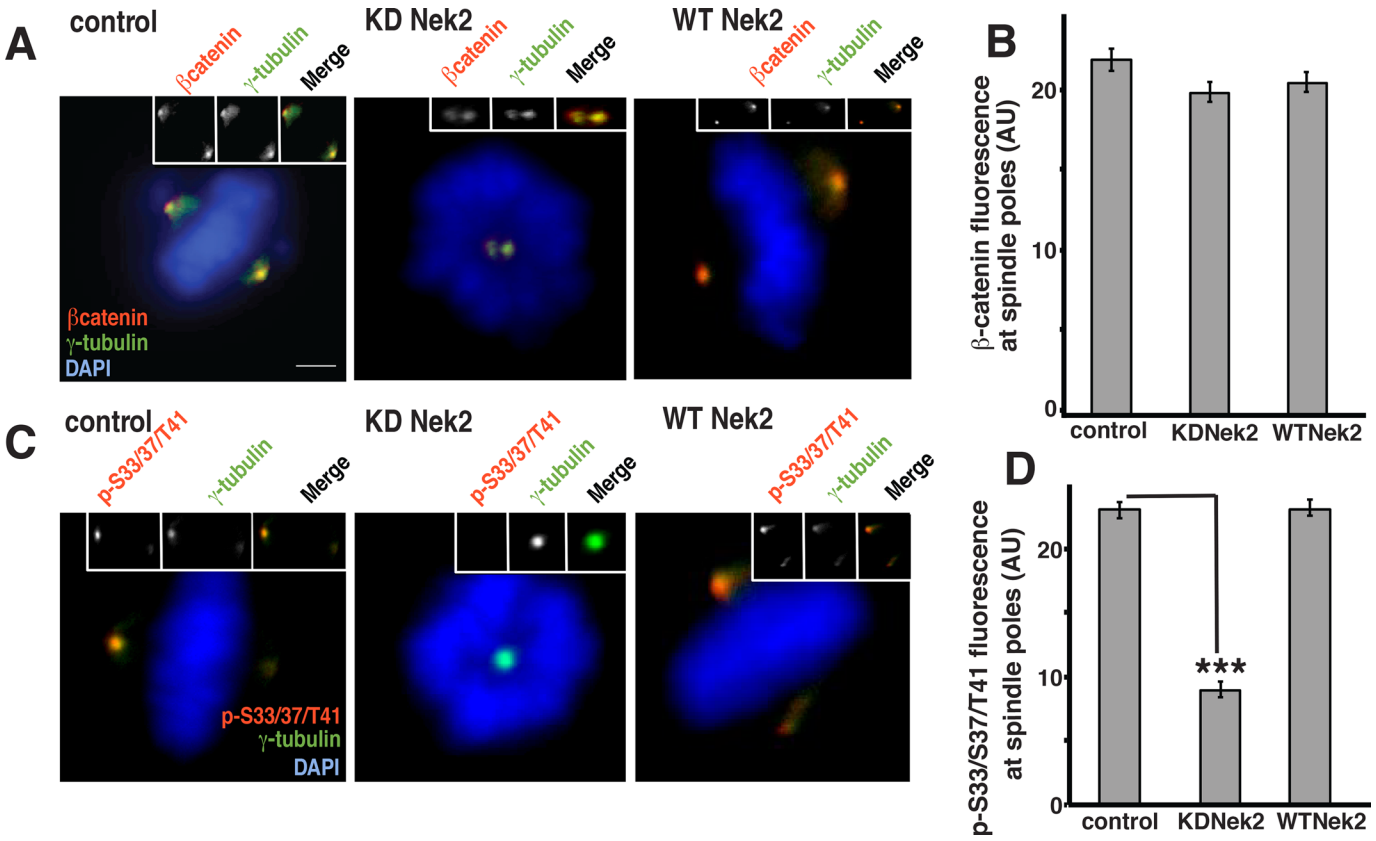

FIGURE 5: Nek2 activity is required for phospho-S33/S37/T41 reactivity at spindle poles (A, C) U2OS cells were synchronized in mitosis by double-thymidine block and release, transfected with HA-KD Nek2 or HA-WT Nek2, and immunostained with antibodies as indicated. For presentation of control spindles and different treatments, images were taken at identical exposure times and identically contrast enhanced for each stain. Scale bar, 10 μm. (B, D) Levels of β-catenin (B) and phospho-S33/S37/T41 immunofluorescence (D; AU, arbitrary units) at spindle poles of untreated U2OS cells or cells treated as described in A and C. Error bars, SEM of ≥15 spindle poles for B and SEM of ≥15 spindle poles for D per experiment from two experiments; ***$p < 0.001$. Original unmodified images taken at identical exposure times were measured for controls and transfected cells.

spindles compared with control spindles, indicating that maximal phospho-S33/S37/T41 reactivity is obtained by endogenous Nek2 activity and cannot be further increased by overexpressing Nek2. These results also show that the reduction of phospho-S33/S37/T41 reactivity in HA-KD-Nek2–transfected cells is specific for KD-Nek2 and not induced by synchronization or transfection protocols.

These results show that Nek2 activity is required for the majority of phospho-S33/S37/T41 reactivity at mitotic spindle poles and has little or no effect on total β-catenin levels. Thus β-catenin localized at these poles independently of phosphorylation (see *Discussion* and schematic in Figure 8C later in the article).

Plk1 activity regulates levels of phospho-S33/S37/T41 reactivity at spindle poles

Nek2 activity at centrosomes is regulated by Plk1 at the onset of mitosis (Mardin *et al.*, 2011). To test whether Plk1 regulates phospho-S33/S37/T41 reactivity at spindle poles, we synchronized U2OS cells in mitosis by double-thymidine block and release in the presence of Plk1 inhibitor BI2536 (Lenart *et al.*, 2007; Steegmaier *et al.*, 2007) or, as controls, in the presence of DMSO, the Eg5 kinesin inhibitor monastrol (Kapoor *et al.*, 2000), or GSK3 inhibitor SB21673. Mitotic cells were immunostained for β-catenin or phospho-S33/37/T41 and coimmunostained for the microtubule marker α-tubulin and centrosomal marker γ-tubulin. We measured the mean fluorescence intensity of β-catenin and phospho-S33/S37/T41 at bipolar spindle poles of cells treated with DMSO or GSK3β inhibitor and at monopolar spindle poles induced by Plk1 inhibitor or Eg5 inhibitor (Figure 6).

Plk1 inhibition significantly reduced γ-tubulin localization to the centrosome and reduced microtubule minus-end focusing at the pole (Figures 6 and 7), which is consistent with a previous study (Haren *et al.*, 2009). Localization of PCM component pericentrin was less affected (Figure 7), indicating that PCM structure is not fully disrupted. The level of β-catenin at the spindle poles was not affected by Plk1 inhibition (Figure 6, B, second from top, and C), whereas there was a statistically significant decrease in phospho-S33/S37/T41 reactivity (~49%) compared with control bipolar spindle poles (Figure 6, D, second from top, and E). Note that immunofluorescence staining of individual spindle poles could not be measured separately in most of the monopolar spindles in the presence of the Plk1 because individual poles were not resolved, which likely masked the overall reduction in phospho-S33/S37/T41 reactivity. However, the decrease in phospho-S33/S37/T41 reactivity at Plk1-inhibited monopolar spindle poles did not cause a corresponding decrease in total β-catenin levels, indicating that β-catenin localized at these poles independently of phosphorylation (see *Discussion* and schematic in Figure 8C).

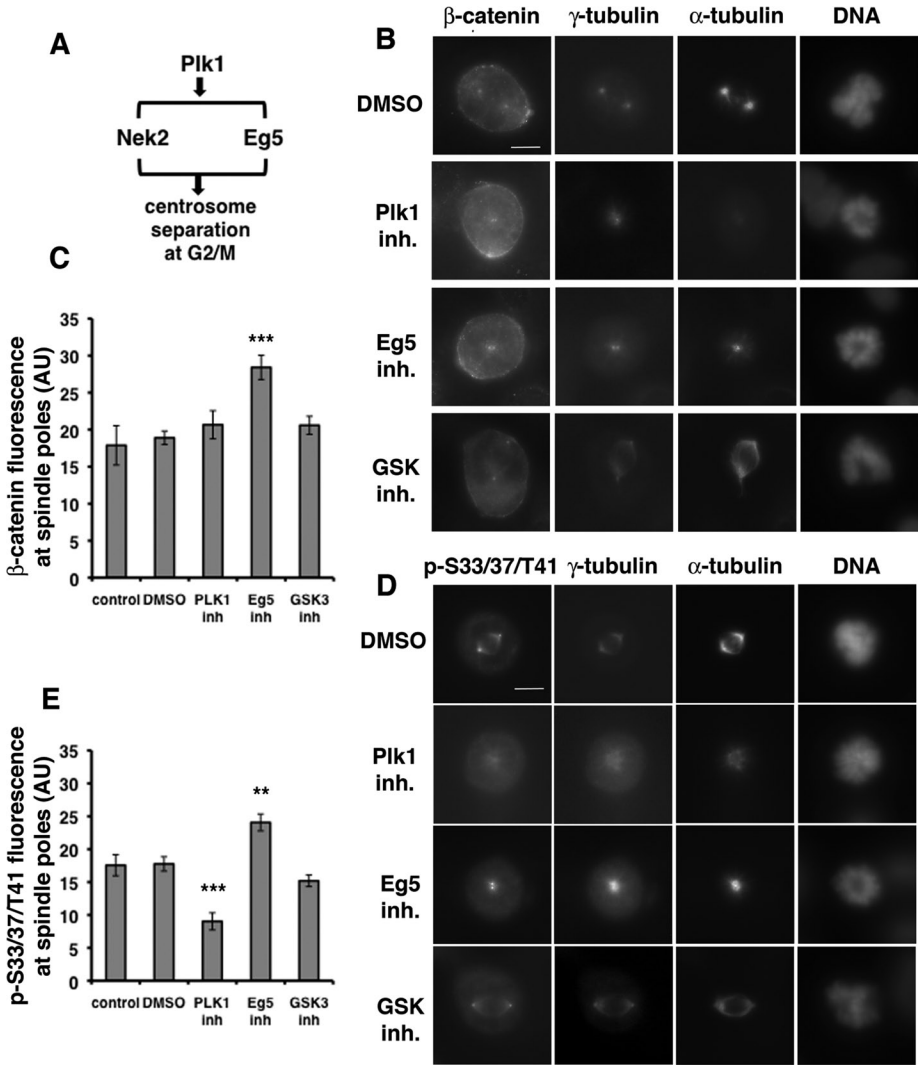

FIGURE 6: Plk1 activity regulates phospho-S33/S37/T41 reactivity at spindle poles. (A) Pathways for regulation of centrosome separation by Plk1 at the onset of mitosis. (B, D) U2OS cells synchronized in mitosis by double-thymidine block and release were treated with control (2% DMSO), Plk1 inhibitor (100 nM BI2536), Eg5 inhibitor (100 μM monastrol), or GSK3 inhibitor (20 μM SB21673) for the last 9 h of the second release, stained for DNA with DAPI, and immunostained with antibodies as indicated. For presentation of control spindles and different treatments, images were taken at identical exposure times and identically contrast enhanced for each stain. Scale bar, 10 μm. (C, E) Graphs show levels of β-catenin (C) and phospho-S33/S37/T41 immunofluorescence (E; AU, arbitrary units) at spindle poles of untreated U2OS cells or cells treated as described in B and D. Error bars, SEM of ≥16 spindle poles for C and SEM of ≥10 spindle poles for E; ***$p < 0.001$. Original unmodified images taken at identical exposure times were measured for controls and different treatments. The data are representative of two independent experiments done with all cell lines under identical conditions.

The levels of total β-catenin and phospho-S33/S37/T41 reactivity increased at the poles of monopolar spindles induced by Eg5 inhibitor monastrol (Figure 6, B and D, second from bottom, and C and E) compared with bipolar control spindle poles. Similar to Plk1-induced monopolar spindles, poles in most of the monastrol-induced monopolar spindles could not be measured separately, which likely caused the less-than-twofold increase in intensities compared with the single poles of bipolar spindles. Inhibition of Eg5 kinesin with monastrol does not affect Nek2 activity at spindle poles (Mardin *et al.*, 2010) and therefore did not inhibit β-catenin localization or phosphorylation at spindle poles in our experiments.

Bipolar spindles treated with the GSK3 inhibitor SB21673 did not have a statistically significant decrease of β-catenin or phospho-S33/S37/T41 reactivity compared with control spindles (Figure 6, B and D, bottom, and C and E).

Taken together, these results show that Plk1 activity is required for the majority of phospho-S33/S37/T41 reactivity at mitotic spindle poles and confirm in a different cell line that GSK3β activity does not have a major effect on levels of phospho-S33/S37/T41 reactivity at mitotic spindle poles.

Overexpression of Nek2 rescues Plk1 reduction of levels of phospho-S33/S37/T41 reactivity at spindle poles

Because Plk1 regulated levels of phospho-S33/S37/T41 reactivity at mitotic spindle poles, we tested whether Plk1 regulation is upstream of Nek2. We tested this possibility by determining whether overexpression of Nek2 could rescue phospho-S33/S37/T41 levels at spindle poles in Plk1-inhibited HCT116 $18^{-/\Delta S45}$ cells synchronized in mitosis. Mitotic cells were coimmunostained with the phospho-S33/37/T41 antibody and antibodies to α-tubulin and the centrosome marker γ-tubulin, and the mean fluorescence intensity of phospho-S33/S37/T41 reactivity was measured at spindle poles. Plk1-inhibited cells transiently transfected with Nek2 showed a statistically significant increase in the mean fluorescence intensity of phospho-S33/S37/T41 reactivity compared with untransfected Plk1-inhibited cells (Figure 7, A, second from bottom, and B). In addition, we observed a small increase in the distance between the spindle poles. Expression of KD Nek2 in Plk1-inhibited cells did not affect the mean fluorescence intensity of phospho-S33/S37/T41 reactivity compared with untransfected Plk1-inhibited cells (Figure 7, A, bottom, and B). In summary, overexpression of active but not KD Nek2 rescued the level of phospho-S33/S37/T41 reactivity at mitotic spindle poles in Plk1-inhibited cells.

C-Nap1 is phosphorylated by Nek2 and removed from centrosomes at the G2/M transition when Nek2 activity is increased (Fry *et al.*, 1998). Therefore we used C-Nap1 removal at mitotic spindle poles to verify that expression of Nek2 indeed rescued the effects of Plk1 inhibition. In control cells treated with 0.2% DMSO, C-Nap1 was not detected at mitotic spindle poles (Figure 7C, top). In Plk1-inhibited cells, C-Nap1 levels remained high at mitotic spindle poles and at the poles of monopolar spindles (Figure 7C, second from top; Mardin *et al.*, 2011). In Plk1-inhibited cells transiently transfected with Nek2, the poles of monopolar spindles did not contain C-Nap1 (Figure 7C, second from bottom), indicating that Nek2 rescue had occurred. However, Nek2 rescue was not complete, as there was only partial separation of

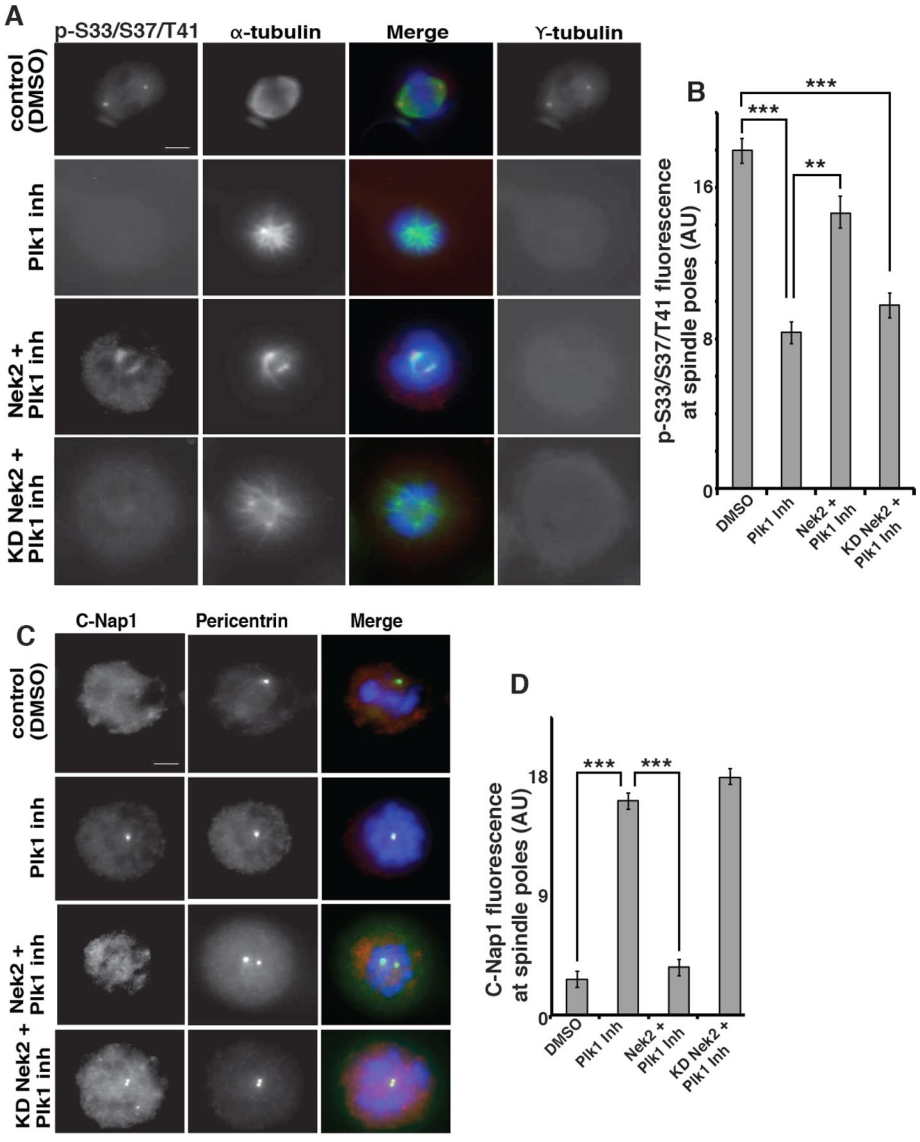

FIGURE 7: Nek2 rescues Plk1 inhibition of phospho-S33/S37/T41 reactivity at spindle poles. (A) HCT116 $18^{-/\Delta S45}$ cells were synchronized in mitosis by double-thymidine block and release and were transfected as indicated. Cells were treated with control (2% DMSO) or Plk1 inhibitor (100 nM BI2536) for 6 h, processed for immunofluorescence with antibodies as indicated, and stained for DNA with DAPI. For presentation of control spindles and different treatments, images were taken at identical exposure times and identically contrast enhanced for each stain. Scale bar, 10 μm. (B) Quantitation of phospho-S33/S37/T41 reactivity at spindle poles (AU, arbitrary units); error bars, SEM of ≥15 spindle poles (***p <0.001; **p < 0.01) per experiment from two experiments. Original unmodified images taken at identical exposure times were measured for controls and different treatments. (C) HCT116 $18^{-/\Delta S45}$ cells treated as described in A were processed for immunofluorescence with antibodies as indicated. Images were taken and prepared as described for A. Scale bar, 10 μm. (D) Quantitation of C-Nap1 levels at spindle poles; error bars, SEM of ≥15 spindle poles per experiment from two experiments (***p < 0.001). Original unmodified images taken at identical exposure times were measured for controls and different treatments.

spindle poles, which may be due to the inability of Nek2 overexpression to rescue Plk1-induced Eg5 localization to spindles (Mardin *et al.*, 2011). Expression of KD Nek2 in Plk1-inhibited cells also failed to remove C-Nap1 from mitotic spindle poles (Figure 7C, bottom). Thus Plk1 is upstream of Nek2 regulation of centrosome disjunction at the G2/M transition and the increased levels of phospho-S33/S37/T41 reactivity at mitotic spindle poles.

Plk1 activity regulates levels of phospho-S33/37/T41 β-catenin

To determine whether Plk1 is involved in the regulation of the phosphorylation of β-catenin at S33/S37/T41, we used the phospho-S33/37/T41 antibody to immunoprecipitate proteins from HCT116 $18^{-/\Delta S45}$ cells synchronized in mitosis and treated with either DMSO or the Plk1 inhibitor BI2536. Immunoprecipitates were immunoblotted with β-catenin and phospho-S33/S37/T41 specific antibodies (Figure 8). The level of phospho–β-catenin immunoprecipitated from mitotic cells was 70% higher than the level from asynchronous cells, although the level of β-catenin in whole-cell lysates was the same (Figure 8, A and B). Significantly, there was a decrease in phospho-S33/37/T41 β-catenin levels immunoprecipitated from lysates of Plk1-inhibited mitotic cells compared with untreated mitotic cells (Figure 8, A and B). We conclude that β-catenin phosphorylation at S33/S37/T41 in mitotic cells requires Plk1 activity.

DISCUSSION

β-Catenin is a multifunctional protein and has been studied extensively in the context of its roles in cell–cell adhesion and Wnt signaling (Nelson and Nusse, 2004). However, there is accumulating evidence for a role of β-catenin in centrosome disjunction and bipolar spindle formation (Kaplan *et al.*, 2004; Bahmanyar *et al.*, 2008; Chilov *et al.*, 2011).

In this study, we sought to dissect mechanisms that regulate β-catenin at centrosomes during mitosis. Our analysis focused on a key step in the regulation of β-catenin levels that involves phosphorylation of S33/S37/T41 in the N-terminus of β-catenin. Normally, phosphorylation of these sites by GSK3β results in β-catenin ubiquitination and degradation by the proteasome (Hart *et al.*, 1999). However, it has been concluded from immunofluorescence studies that levels of phospho-S33/S37/T41 β-catenin increase rather than decrease at mitotic spindle poles (Huang *et al.*, 2007). We resolved this contradiction by showing that Nek2 activity, not GSK3β activity, is required for the majority of phospho-S33/S37/T41 reactivity and for phospho-S33/S37/T41 β-catenin at mitotic spindle poles. Furthermore, we showed that Nek2 inhibits binding of the E3 ligase, β-TrCP, to β-catenin and hence inhibits β-catenin ubiquitination and degradation and that Nek2 regulation of phospho-S33/S37/T41 reactivity at spindle poles is downstream of Plk1 activity.

S33/S37/T41 and at least five additional residues in β-catenin are specifically phosphorylated by Nek2, based on LC-MS/MS of β-catenin phosphorylated in vitro by Nek2 and recognition by the phospho-S33/S37/T41 antibody. Nek2 phosphorylation of S33/S37/

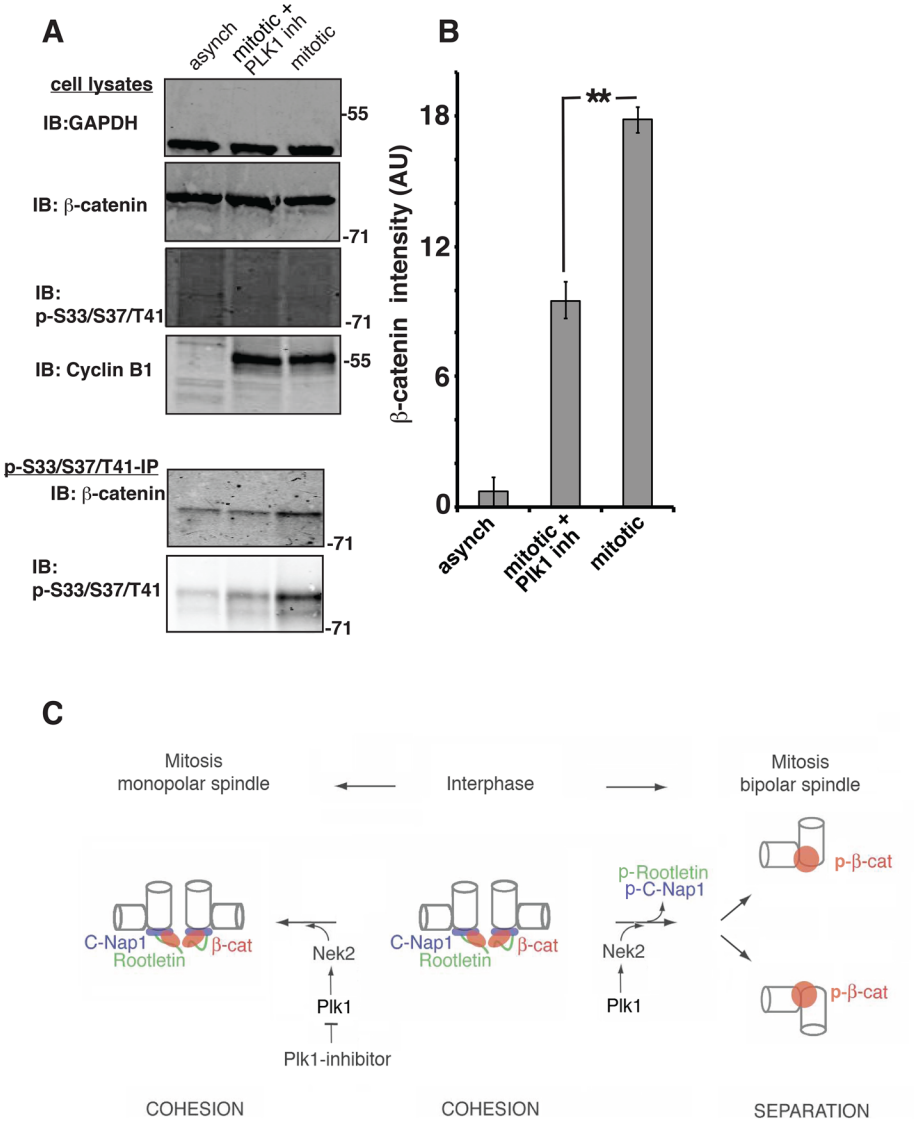

FIGURE 8: Plk1 activity regulates phospho-S33/S37/T41 β-catenin levels. (A) HCT116 $18^{-/\Delta S45}$ cells were synchronized in mitosis and treated with control (2% DMSO) or Plk1 inhibitor (100 nM BI2536). Whole-cell lysates were immunoblotted for glyceraldehyde-3-phosphate dehydrogenase, β-catenin, phospho-S33/S37/T41 β-catenin, and cyclin B1. Cell lysates were immunoprecipitated with the phospho-S33/37/T41 antibody and immunoprecipitates immunoblotted for β-catenin and phospho-S33/S37/T41 reactivity. Phospho-S33/S37/T41 β-catenin is detectable only after concentrating it by immunoprecipitation (30 µl of total lysate/lane vs. immunoprecipitate from 500 µl of total lysate/lane was loaded). (B) Quantitation of phospho–β-catenin band intensities as measured in the immunoblots of β-catenin coimmunoprecipitated with the phospho-S33/S37/T41 antibody (AU, arbitrary units); error bars, SEM of three independent experiments (**$p < 0.008$). (C) Model for regulation of Nek2 by Plk1 at the onset of mitosis, which results in removal of centrosomal linker proteins C-Nap1 and rootletin and activation of phospho-S33/S37/T41 β-catenin. Localization of β-catenin to interphase centrosomes is mediated by the linker proteins C-Nap1 and rootletin. At the onset of mitosis, activation of Plk1 and Nek2 at centrosomes leads to phosphorylation of the linker proteins and β-catenin. The linker proteins are removed from centrosomes, whereas phospho–β-catenin (p-β-cat) remains associated with the spindle poles. In monopolar spindles caused by inhibition of Plk1 the linker proteins are not removed and continue to provide binding sites for nonphosphorylated β-catenin at the spindle pole.

T41 is surprising since previous results implied that Nek2 stabilizes β-catenin at centrosomes (Bahmanyar *et al.*, 2008), whereas S33/S37/T41 phosphorylation by GSK3β results in β-catenin ubiquitination and degradation (Hart *et al.*, 1999). However, we found that the level of ubiquitinated β-catenin in cells overexpressing Nek2 is reduced. Surprisingly, we found the same effect with KD Nek2, although other kinases have not been shown to bind directly to β-catenin independently of phosphorylation (Piedra *et al.*, 2001; Gao *et al.*, 2002; Zhang *et al.*, 2003; Hino *et al.*, 2005; Kim *et al.*, 2010). Significantly, since both Nek2 and KD Nek2 coimmunoprecipitated with β-catenin, a multiprotein scaffolding interaction (Mardin *et al.*, 2011) or direct binding of these proteins could block binding of the E3 ligase, β-TrCP, to β-catenin, consistent with β-catenin not being ubiquitinated or degraded. However, further work is needed to fully test this model.

To test directly whether GSK3β-independent S33/S37/T41 phosphorylation of β-catenin occurred at centrosomes, we enriched centrosomes from HCT116 $18^{-/\Delta S45}$ cells in which the wild-type β-catenin allele was deleted and the other allele contained a β-catenin mutant with the in-frame deletion of S45; S45 is the CK1 priming site required for subsequent GSK3β phosphorylation of S33/S37/T41 (Liu *et al.*, 2002). We observed a significant increase in levels of phospho-S33/S37/T41-β-catenin in centrosomes from mitotic HCT116 $18^{-/\Delta S45}$ cells compared with asynchronous cells. This result confirmed that β-catenin is phosphorylated at S33/S37/T41 sites at centrosomes during mitosis and that GSK3β activity cannot be involved. In addition, we showed in two independent cell lines (HCT116 $18^{-/\Delta S45}$ and U2OS) that GSK3β inhibition had no effect on phospho-S33/S37/T41 reactivity at spindle poles but that Nek2 activity was required. In summary, our data show that phospho-S33/S37/T41 β-catenin is enriched at mitotic centrosomes and that the majority of phospho-S33/S37/T41 reactivity at spindle poles is generated by Nek2 activity and not GSK3β.

Centrosome enrichment from cell lysates requires depolymerization of microtubules. Thus phospho–β-catenin that cofractionated with mitotic centrosomes was associated with centrosomes independently of microtubules. We observed a high–molecular weight protein in Western blots for phospho-S33/S37/T41 in sucrose gradient fractions from mitotic and asynchronous cells. This protein did not peak with Aurora A, γ-tubulin, or β-catenin (Figure 3, A and B), indicating that it was not closely associated with β-catenin or centrosomes, although it is possible that microtubule depolymerization affected the interaction of this protein with centrosomes. We also observed additional high–molecular weight protein(s) in Western blots of mitotic extracts and microtubule-dependent reactivity at spindle poles with the phospho-S33/S37/T41 antibody (M.B. and

A.I.M.B., unpublished results). Thus the phospho-S33/S37/T41 antibody may react with similar epitopes in other mitotic and/or spindle pole proteins in addition to phospho-S33/S37/T41 β-catenin. Further studies are needed to identify these additional proteins.

We confirmed that Nek2 phosphorylates S33/S37/T41 in β-catenin by inhibiting Nek2 activity with Plk1. This inhibition did not affect total β-catenin levels but decreased the level of phospho-S33/S37/T41 β-catenin in extracts from mitotic HCT116 $18^{-/\Delta S45}$ cells and decreased phospho-S33/S37/T41 reactivity at spindle poles. In addition, overexpressed Nek2 rescued this phenotype by accumulating phospho-S33/S37/T41 reactivity at spindle poles during mitosis and initiating centrosome disjunction. Centrosome separation was only partially rescued by Nek2 because there is a parallel Plk1-dependent pathway mediated by Eg5, which does not require Nek2 and is required for formation of bipolar spindles (Mardin *et al.*, 2011). Thus we conclude that Plk1 is upstream of Nek2 in increasing phospho-S33/S37/T41 reactivity at spindle poles and the level of phospho-S33/S37/T41 β-catenin in mitotic cells (Figure 8C).

Our previous results (Bahmanyar *et al.*, 2008) indicated that there are two mechanisms of β-catenin localization to centrosomes: 1) β-catenin localization to interphase centrosomes is mediated by the linker proteins rootletin and C-Nap1; and 2) at the onset of mitosis, β-catenin localization becomes independent of these linker proteins but dependent on Nek2 activity (Bahmanyar *et al.*, 2008; Figure 8C). The linker is not removed from poles of monopolar spindles in cells overexpressing KD Nek2 or treated with Plk-1 inhibitor (Figure 7; Mardin *et al.*, 2011). Therefore linker-protein–dependent localization of β-catenin is likely preserved at these poles. This explains why total β-catenin levels are little affected by inhibition of Nek2 or Plk1 activity, although β-catenin phosphorylation is inhibited (see schematic in Figure 8C).

In summary, we identified a novel signaling pathway at mitotic spindle poles that is involved in promoting centrosome disjunction. We showed that Nek2 is the main regulator of β-catenin at centrosomes and that β-catenin phosphorylation is independent of GSK3β. We showed a Nek2-mediated mechanism for centrosome disjunction by retaining β-catenin at the centrosome during mitosis rather than removing it, as is the case of C-Nap1 and rootletin (Faragher and Fry, 2003). It remains unclear how β-catenin promotes centrosome disjunction or what role the phosphorylated stabilized pool of β-catenin plays at centrosomes. It is also not clear whether Nek2 phosphorylation mainly protects β-catenin against the destabilizing phosphorylation by GSK3β/CK1 or whether the Nek2 phospho sites are more directly required for β-catenin function. Previously published results indicate that expression of phospho-mutant β-catenin is sufficient to induce centrosome disjunction (Bahmanyar *et al.*, 2008; Hadjihannas *et al.*, 2010). However, expression of phospho-mimic β-catenin is required in neuronal progenitors to maintain γ-tubulin and microtubules at centrosomes (Chilov *et al.*, 2011). This indicates that β-catenin stability may be sufficient for some functions, such as removal of the linker proteins cNap-1 and rootletin, and that phospho sites may be required for others, such as γ-tubulin recruitment and centrosome maturation. APC and other β-catenin interactors are present at centrosomes (Louie *et al.*, 2004; Hadjihannas *et al.*, 2006, 2010), but they have been studied only in the context of phosphorylation by GSK3β/CK1 and not Nek2. β-Catenin has additional Nek2 phosphorylation sites that may affect the interaction of β-catenin with binding partners differently than phosphorylation by GSK3β/CK1. In summary, β-catenin may regulate centrosome disjunction at the onset of mitosis by more than one mechanism that probably involves changes in its interaction with centrosome multiprotein complexes. Future experiments to modify the pathway regulating β-catenin phosphorylation at mitotic centrosomes, combined with biochemical analysis of β-catenin protein complexes in enriched mitotic centrosome preparations, will allow us to further characterize the role of β-catenin phosphorylation by Nek2 in centrosome disjunction.

MATERIALS AND METHODS

Cell lines and inhibitors

HEK293T cells were grown in DMEM supplemented with 10% fetal bovine serum (FBS). U2OS cells were grown in McCoy's 5A medium (Life Technologies, Gibco, Grand Island, NY) supplemented with 10% FBS. U2OS have been described previously (Chang and Stearns, 2000; Bahmanyar *et al.*, 2008). HCT116 parental line and HCT116 cell lines derived from these by somatic cell gene targeting were a gift from Todd Waldman (Georgetown University School of Medicine, Washington, DC) and grown as described (Kim *et al.*, 2002a,b). For transient transfection of cDNAs, Lipofectamine 2000 reagent was used as described by the manufacturer (Life Technologies, Invitrogen, Grand Island, NY). For experiments in Figure 1D, HEK293T cells were transfected with GFP–β-catenin or GFP–β-catenin and HA–Nek2 or HA–KD–Nek2. At 48 h after transfection, cells were extracted with 1% SDS buffer, and equivalent amounts of protein were subjected to SDS–PAGE and Western blotting. For experiments in Figure 4, HCT116 cell lines were cultured for 24 h on collagen-coated coverslips, fixed, and stained as described later, or treated for 4 h before fixation with 0.2% DMSO or the following GSK3 inhibitors: 20 μM SB216763 (Sigma-Aldrich, St. Louis, MO), 5 μM GSK-3 inhibitor IX (EMD Chemicals, Billerica, MA), or 20 mM LiCl (Sigma-Aldrich). For experiments shown in Figures 5–7, cells were incubated with 2.5 mM thymidine for 16–18 h (HCT116 cells) or 24 h (U2OS cells), then thymidine was washed out three times, and cells were incubated without thymidine for 5 h (HCT116) or 10 h (U2OS); cells were reincubated with 2.5 mM thymidine for another 16–18 h (HCT116 cells) or 20 h (U2OS cells). Thymidine was washed out, and cells were plated onto coverslips for another 5 h (HCT116 cells) or 12 h (U2OS cells) for release into mitosis. DMSO (0.2%), the Plk1 inhibitor BI 2536 (100 nM; ChemieTek, Indianapolis, IN), the Eg5 inhibitor monastrol (100 μM; Sigma-Aldrich), or the GSK3 inhibitor SB 21673 (20 μM) was added to some of the synchronized U2OS cells for 9 h at the end of the second release. For experiments shown in Figure 8, HCT116 $18^{-/\Delta S45}$ cells were synchronized in G2/M with the Cdk1 inhibitor RO-3306 (9 μM) for 18 h and released for 2 h with or without Plk1 inhibitor BI 2536 (100 nM) for the last 6 h.

DNA constructs

GFP–β-catenin and GFP–β-catenin with S33/S37/T41/S45 → A mutations were described previously (Bahmanyar *et al.*, 2010). HA-WT and KD-Nek2 (Eto *et al.*, 2002) constructs were a gift from D. Brautigan (University of Virginia, Charlottesville, VA). HA-ubiquitin (Deng *et al.*, 2000) was a gift from Zhijian Chen at University of Texas Southwestern Medical Center (Dallas, TX). The Myc–β-TrCP plasmid (Ohta and Xiong, 2001) was obtained from Addgene (Cambridge, MA; Addgene plasmid 20718). GST-N-terminal-β-catenin construct was a gift from W. Weis (Stanford University, Stanford, CA). GST and GST-N-terminal-β-catenin were prepared as described previously (Huber *et al.*, 1997).

Cell fixation, antibodies, and fluorescence quantitation

Cells were fixed in –20°C methanol as described previously (Louie *et al.*, 2004). The following antibodies were used: rabbit polyclonal β-catenin, 1:200 (Nathke *et al.*, 1994); mouse monoclonal γ-tubulin clone GTU88, 1:50 (Sigma-Aldrich); rabbit polyclonal pericentrin,

1:200 (Covance, Princeton, NJ); mouse monoclonal C-Nap1, 1:200 (BD Transduction Laboratories, San Jose, CA); mouse monoclonal Nek2, 1:200 (BD Transduction Laboratories); rabbit anti–phospho-S33/S37/T41 β-catenin, 1:200 (overnight incubation; 9561; Cell Signaling Technology, Danvers, MA); and rat anti–α-tubulin YL1/2, 1:2000 (SC-53029; Santa Cruz Biotechnology, Dallas, TX). The phospho-S33/S37/T41 antibody was raised against a phospho-S33/S37/T41 peptide and has been used in a large number of studies by many laboratories. The antibody recognizes N-terminal amino acids in β-catenin that are directly phosphorylated by GSK3β. This is supported by work from our laboratory: 1) the antibody does not recognize a mutant β-catenin containing alanine substitutions of S33/S37/T41/S45 (GFP-β-catenin* in Figure 1D; Harris and Nelson, 2010; 2) the antibody does not recognize β-catenin that has been treated with λ-phosphatase (Harris and Nelson, 2010); and 3) specific inhibition of GSK3β results in loss of phospho-S33/S37/T41 antibody recognition of β-catenin (Supplemental Figure S4). Secondary antibodies against rabbit, rat, or mouse immunoglobulin G (IgG) with minimal species cross-reactivity and coupled to fluorescein isothiocyanate (FITC), rhodamine, Alexa 647, or Cy5 were used at a dilution of 1:200 for FITC and rhodamine, 1:100 for Cy5, and 1:100 for Alexa 647 (111-295-144, 111-095-144, 111-605-144, or 111-175-144 goat anti-rabbit; 112-095-167, 112-295-167, or 112-605-167 goat anti-rat; and 115-295-166, 115-095-166 or 115-605-166 goat anti-mouse; Jackson ImmunoResearch Laboratories, West Grove, PA). These antibodies were used for triple or quadruple costains in combination with 4′,6-diamidino-2-phenylindole (DAPI) as a DNA stain.

Epifluorescence was analyzed using a Zeiss Axioplan microscope (Carl Zeiss Meditec, Dublin, CA) with the following filter set: DAPI (Chroma 31000v2), FITC (Omega XF22), rhodamine (Omega XF37), Cy5 (Chroma 41008), as described elsewhere (Louie *et al.*, 2004). Epifluorescence of metaphase spindle poles or of monopolar spindle poles were analyzed, and fluorescence intensity at spindle pole bodies was measured as described before for interphase centrosomes (Bahmanyar *et al.*, 2010). Briefly, images were recorded using identical exposure times for each fluorescence staining and analyzed using ImageJ (National Institutes of Health, Bethesda, MD). Mean fluorescence intensity was measured at spindle poles marked by costaining with γ-tubulin and corrected for background fluorescence intensity of an equivalent area next to each spindle pole. For statistical evaluation of fluorescence quantitations by Mann–Whitney test, LiCl-treated cells were compared with untreated cells, and cells treated with inhibitors in DMSO (SB21673, GSK3 inhibitor IX, PLK1 inhibitor BI2536) were compared with cells treated with equivalent concentrations of DMSO.

Immunoprecipitation of β-catenin, ubiquitin, β-TrCP, and phospho-S33/S37/T41 β-catenin

HEK293T cells (transfected with GFP–β-catenin in the case of β-catenin/ubiquitin/Nek2 coimmunoprecipitations) were extracted in cold lysis/IP buffer (20 mM Tris-HCl, pH 7.5, 120 mM NaCl, 1 mM EDTA, 1 mM ethylene glycol tetraacetic acid [EGTA], 1 mM dithiothreitol [DTT], and 0.5% NP-40 containing Complete EDTA-free Protease Inhibitor Cocktail [Roche Diagnostics GmbH, Mannheim, Germany] and phosphatase inhibitor cocktails 1 and 2 [Sigma-Aldrich]), and lysed using a Dounce homogenizer. Nuclei and unbroken cells were pelleted, and the postnuclear supernatant was precleared by incubation with protein A (rabbit antibody) or protein G (mouse antibody) Sepharose 4B (GE Healthcare Biosciences, Uppsala, Sweden) and rabbit or mouse serum. For Usp2 treatments of immunoprecipitates, antibody–protein complexes isolated on protein A (rabbit antibody) or protein G (mouse antibody) Sepharose 4B beads in IP buffer were incubated with Usp2 (5 μg; Baker *et al.*, 2005) at 37°C for 30 min to remove HA-ubiquitin. Beads were washed four times using lysis/IP buffer with 500 mM NaCl and denatured in Laemmli sample buffer. Precipitated proteins were separated using SDS–PAGE and analyzed by Western blotting. The same protocol was followed for the β-catenin/β-TrCP/Nek2 coimmunoprecipitations using anti-Myc 9E10 or polyclonal β-catenin antibody. Phospho–β-catenin was immunoprecipitated from NP40 extracts from asynchronous or synchronized HCT116 $18^{-/\Delta S45}$ cells with phospho-S33/S37/T41 β-catenin antibody (rabbit anti–phospho-S33/S37/T41 β-catenin 561; Cell Signaling Technology) by overnight incubation at 4°C and coupling to protein A Sepharose 4B (GE Healthcare). Immunoprecipitates were washed four times in IP buffer and centrifuged at 3000 rpm for 2 min and then denatured in Laemmli sample buffer. Precipitated proteins were separated by SDS–PAGE and analyzed by Western blotting.

Kinase assays

For kinase assays, 100 ng of GSK3β/CK1α (a gift of W. Weis) were incubated with 300 nM recombinant GST-N-terminal-β-catenin, 150 nCi/nmol [^{32}P]ATP with a total ATP concentration of 100 nM, and 50 nM microcystin in kinase buffer (50 mM Tris-HCl, pH 7.7, 10 mM $MgCl_2$, 1 mM DTT, and a protease inhibitor cocktail). Kinase reactions were incubated for 60 min at 30°C and denatured in Laemmli sample buffer, followed by SDS–PAGE, and analyzed by Western blotting. Kinase assays using recombinant His-Nek2 were performed as described but with 200 ng of recombinant His-Nek2 (BPS Bioscience, San Diego, CA) per reaction as the source of kinase and 300 nM recombinant GST-N-terminal β-catenin (Huber *et al.*, 1997) as substrate or 300 nM GST as a control substrate.

Centrosome isolation, immunoprecipitation of centrosomal β-catenin, and identification of phospho–β-catenin

Centrosome-enriched fractions were prepared as described previously (Bornens *et al.*, 1987) with modifications as described. HCT116 $18^{-/\Delta S45}$ cells were treated with Cdk1 inhibitor RO-3306 (9 μM) for 18 h (Vassilev *et al.*, 2006) and released for 90 min in the presence of 10 μg/ml nocodazole and 5 μg/ml cytochalasin. Cells were washed and lysed in 0.5% NP-40 buffer, and lysates were loaded onto a discontinuous sucrose gradient as described previously (Bornens *et al.*, 1987). After centrifugation, 24 fractions (500 μm each) were collected from the sucrose gradients, and pairs of fractions were pooled (1+2, 3+4, etc. = 12 fractions), mixed with 8× SDS Laemmli sample buffer, and subjected to SDS–PAGE. Centrosome-containing fractions and noncentrosome fractions were solubilized in IP buffer (20 mM Tris-HCl, pH 7.7, 120 mM NaCl, 1 mM EDTA, 1 mM EGTA, 1 mM DTT, and protease inhibitor cocktail) and precleared by incubation with protein A (rabbit antibody) or protein G (mouse antibody) Sepharose 4B (GE Healthcare) and rabbit or mouse serum. Phospho–β-catenin was immunoprecipitated from the fractions with rabbit phospho-S33/S37/T41–specific antibody (9561; Cell Signaling Technology) as described for HCT116 $18^{-/\Delta S45}$ lysates.

Immunoblotting and quantitation of protein levels

The following antibodies and dilutions were used: rabbit anti-GFP antibody, 1:1000 (Invitrogen); mouse GFP antibody, 1:1000 (Clontech Laboratories, Mountain View, CA); mouse monoclonal anti–β-catenin, 1:1000 (BD Transduction Laboratories); rabbit polyclonal β-catenin 1:1000 (Nathke *et al.*, 1994); γ-tubulin clone GTU88, 1:1000 (Sigma-Aldrich); mouse monoclonal HA.11, 1:1000

(Covance); mouse monoclonal myc 9E10, 1:500 (Santa Cruz Biotechnology); Nek2 mouse monoclonal, 1:500 (BD Transduction Laboratories); rabbit anti–phospho-S33/S37/T41 β-catenin, 1:500 (overnight incubation; 9561; Cell Signaling Technology); and Aurora A rabbit polyclonal, 1:2000 (ab1287; Abcam, Cambridge, MA). Secondary antibodies against mouse or rabbit IgG with minimal cross-reactivity were coupled to either IRDye 800CW (LI-COR, Lincoln, NE) or Alexa Fluor 680 (Invitrogen) and used at a dilution of 1:30,000. Immunoblots were scanned at 680 and 800 nm using an Odyssey infrared imaging system (Li-COR) and quantified with Odyssey software and ImageJ. To quantify β-catenin phosphorylation (S33/S37/T41), the intensity of the bands was normalized to the total GFP–β-catenin intensity (Figure 1) and total β-catenin intensity (Figure 7). For ubiquitinated β-catenin, the entire lane starting at the asterisk of the HA blot was quantified and normalized to the total GFP–β-catenin intensity. For the centrosome fractions, the intensity of the band of each fraction was measured. Significance was calculated using the Mann–Whitney test. Resulting images of entire blots were adjusted using ImageJ and cropped only after all adjustments were performed.

Mass spectrometry

Samples for LC-MS/MS analysis were prepared as follows. Purified β-catenin incubated with Nek2, either with ATP or without for control purposes, was buffer exchanged into 100 mM ammonium bicarbonate with a 30-kDa molecular-weight cutoff spin filter (Millipore) and concentrated into 25 µl. Tryptic digestion was performed in the presence of 25 µl of trifluoroethanol (Sigma-Aldrich) and 2.5 µl of DTT (Sigma-Aldrich). The sample was heated at 90°C for 20 min to denature the protein. Then 10 µl of 200 mM iodoacetamide was added and incubated for 1 h in the dark. we added 300 µl of water and 100 µl of 100 mM ammonium bicarbonate to dilute denaturant. Sequencing-grade trypsin (Promega Corporation, Madison, WI) was added at a ratio of 1:40 and incubated at 37°C overnight. The peptide analysis was performed in positive mode using an Agilent 6520 LC/MS QTOF system equipped with an HPLC-Chip source (Agilent Technologies, Santa Clara, CA).

An Agilent 1200 CapPump was used to load peptides onto the Agilent 1200 ChipCube. An Agilent 1200 NanoPump was used to generate gradient nanoflow at 400 nl/min using typical mobile phases of 0.1% formic acid in MS-grade water (solvent A) and 0.1% formic acid in acetonitrile (solvent B). The peptide mixtures were separated on a 75 µm × 43 mm C18 column. The gradient for separation was 3% B for the first 2 min, 3–45% B over 18 min, and 45–85% B over 2 min, with a hold at 85% B for 3 min, followed by a 85–3% B drop over the last 30 s. The nanoelectrospray voltage was set to 1750 V, with a nitrogen drying gas of 5 l/min at 365°C. The fragmentor voltage was 175 V, and the skimmer voltage was 65 V. Data were acquired at 2 GHz in extended dynamic range mode.

BioConfirm Software (Agilent Technologies) was used to search the MS/MS data against a protein sequence database generated from calculated theoretical masses of the tryptic phosphopeptides. Phosphopeptides were considered to be the result of Nek2 phosphorylation if present in the sample that included ATP but not phosphorylated without ATP.

ACKNOWLEDGMENTS

B.M. is a Howard Hughes Medical Institute Gilliam Fellow, and M.O. gratefully acknowledges financial support from Agilent Technologies. Work from the Nelson laboratory was supported by the National Institutes of Heath (GM35527). We thank William Weis for the GST-N-terminal β-catenin expression vector, Rohan Baker (Australia National University, Canberra, Australia) for pHUsp2-cc, Zhijian Chen for the HA-ubiquitin expression vector, and D. Brautigan for the HA-Nek2 and HA-KD-Nek2 expression vectors.

REFERENCES

Aberle H, Butz S, Stappert J, Weissig H, Kemler R, Hoschuetzky H (1994). Assembly of the cadherin-catenin complex in vitro with recombinant proteins. J Cell Sci 107, 3655–3663.

Arias AM, Brown AM, Brennan K (1999). Wnt signalling: pathway or network? Curr Opin Genet Dev 9, 447–454.

Azimzadeh J, Bornens M (2007). Structure and duplication of the centrosome. J Cell Sci 120, 2139–2142.

Bahe S, Stierhof YD, Wilkinson CJ, Leiss F, Nigg EA (2005). Rootletin forms centriole-associated filaments and functions in centrosome cohesion. J Cell Biol 171, 27–33.

Bahmanyar S, Guiney EL, Hatch EM, Nelson WJ, Barth AI (2010). Formation of extra centrosomal structures is dependent on beta-catenin. J Cell Sci 123, 3125–3135.

Bahmanyar S, Kaplan DD, Deluca JG, Giddings TH Jr, O'Toole ET, Winey M, Salmon ED, Casey PJ, Nelson WJ, Barth AI (2008). beta-Catenin is a Nek2 substrate involved in centrosome separation. Genes Dev 22, 91–105.

Baker RT, Catanzariti AM, Karunasekara Y, Soboleva TA, Sharwood R, Whitney S, Board PG (2005). Using deubiquitylating enzymes as research tools. Methods Enzymol 398, 540–554.

Barth AI, Stewart DB, Nelson WJ (1999). T cell factor-activated transcription is not sufficient to induce anchorage-independent growth of epithelial cells expressing mutant beta-catenin. Proc Natl Acad Sci USA 96, 4947–4952.

Bek S, Kemler R (2002). Protein kinase CKII regulates the interaction of beta-catenin with alpha-catenin and its protein stability. J Cell Sci 115, 4743–4753.

Bornens M, Paintrand M, Berges J, Marty MC, Karsenti E (1987). Structural and chemical characterization of isolated centrosomes. Cell Motil Cytoskeleton 8, 238–249.

Chang P, Stearns T (2000). Delta-tubulin and epsilon-tubulin: two new human centrosomal tubulins reveal new aspects of centrosome structure and function. Nat Cell Biol 2, 30–35.

Chilov D, Sinjushina N, Rita H, Taketo MM, Makela TP, Partanen J (2011). Phosphorylated beta-catenin localizes to centrosomes of neuronal progenitors and is required for cell polarity and neurogenesis in developing midbrain. Dev Biol 357, 259–268.

Deng L, Wang C, Spencer E, Yang L, Braun A, You J, Slaughter C, Pickart C, Chen ZJ (2000). Activation of the IkappaB kinase complex by TRAF6 requires a dimeric ubiquitin-conjugating enzyme complex and a unique polyubiquitin chain. Cell 103, 351–361.

Eto M, Elliott E, Prickett TD, Brautigan DL (2002). Inhibitor-2 regulates protein phosphatase-1 complexed with NimA-related kinase to induce centrosome separation. J Biol Chem 277, 44013–44020.

Faragher AJ, Fry AM (2003). Nek2A kinase stimulates centrosome disjunction and is required for formation of bipolar mitotic spindles. Mol Biol Cell 14, 2876–2889.

Fry AM (2002). The Nek2 protein kinase: a novel regulator of centrosome structure. Oncogene 21, 6184–6194.

Fry AM, Mayor T, Meraldi P, Stierhof YD, Tanaka K, Nigg EA (1998). C-Nap1, a novel centrosomal coiled-coil protein and candidate substrate of the cell cycle-regulated protein kinase Nek2. J Cell Biol 141, 1563–1574.

Fujioka T, Takebayashi Y, Ito M, Uchida T (2000). Nek2 expression and localization in porcine oocyte during maturation. Biochem Biophys Res Commun 279, 799–802.

Gao ZH, Seeling JM, Hill V, Yochum A, Virshup DM (2002). Casein kinase I phosphorylates and destabilizes the beta-catenin degradation complex. Proc Natl Acad Sci USA 99, 1182–1187.

Hadjihannas MV, Bruckner M, Behrens J (2010). Conductin/axin2 and Wnt signalling regulates centrosome cohesion. EMBO Rep 11, 317–324.

Hadjihannas MV, Bruckner M, Jerchow B, Birchmeier W, Dietmaier W, Behrens J (2006). Aberrant Wnt/beta-catenin signaling can induce chromosomal instability in colon cancer. Proc Natl Acad Sci USA 103, 10747–10752.

Ha Kim Y, Yeol Choi J, Jeong Y, Wolgemuth DJ, Rhee K (2002). Nek2 localizes to multiple sites in mitotic cells, suggesting its involvement in

multiple cellular functions during the cell cycle. Biochem Biophys Res Commun 290, 730–736.
Haren L, Stearns T, Luders J (2009). Plk1-dependent recruitment of gamma-tubulin complexes to mitotic centrosomes involves multiple PCM components. PLoS One 4, e5976.
Harris ES, Nelson WJ (2010). Adenomatous polyposis coli regulates endothelial cell migration independent of roles in beta-catenin signaling and cell-cell adhesion. Mol Biol Cell 21, 2611–2623.
Hart M *et al.* (1999). The F-box protein beta-TrCP associates with phosphorylated beta-catenin and regulates its activity in the cell. Curr Biol 9, 207–210.
Hino S, Tanji C, Nakayama KI, Kikuchi A (2005). Phosphorylation of beta-catenin by cyclic AMP-dependent protein kinase stabilizes beta-catenin through inhibition of its ubiquitination. Mol Cell Biol 25, 9063–9072.
Huang P, Senga T, Hamaguchi M (2007). A novel role of phospho-beta-catenin in microtubule regrowth at centrosome. Oncogene 26, 4357–4371.
Huber AH, Nelson WJ, Weis WI (1997). Three-dimensional structure of the armadillo repeat region of beta-catenin. Cell 90, 871–882.
Huelsken J, Behrens J (2002). The Wnt signalling pathway. J Cell Sci 115, 3977–3978.
Kaplan DD, Meigs TE, Kelly P, Casey PJ (2004). Identification of a role for beta-catenin in the establishment of a bipolar mitotic spindle. J Biol Chem 279, 10829–10832.
Kapoor TM, Mayer TU, Coughlin ML, Mitchison TJ (2000). Probing spindle assembly mechanisms with monastrol, a small molecule inhibitor of the mitotic kinesin, Eg5. J Cell Biol 150, 975–988.
Kim EA, Kim JE, Sung KS, Choi DW, Lee BJ, Choi CY (2010). Homeodomain-interacting protein kinase 2 (HIPK2) targets beta-catenin for phosphorylation and proteasomal degradation. Biochem Biophys Res Commun 394, 966–971.
Kim JS, Crooks H, Dracheva T, Nishanian TG, Singh B, Jen J, Waldman T (2002a). Oncogenic beta-catenin is required for bone morphogenetic protein 4 expression in human cancer cells. Cancer Res 62, 2744–2748.
Kim JS, Crooks H, Foxworth A, Waldman T (2002b). Proof-of-principle: oncogenic beta-catenin is a valid molecular target for the development of pharmacological inhibitors. Mol Cancer Ther 1, 1355–1359.
Kuriyama R, Bettencourt-Dias M, Hoffmann I, Arnold M, Sandvig L (2009). Gamma-tubulin-containing abnormal centrioles are induced by insufficient Plk4 in human HCT116 colorectal cancer cells. J Cell Sci 122, 2014–2023.
Lenart P, Petronczki M, Steegmaier M, Di Fiore B, Lipp JJ, Hoffmann M, Rettig WJ, Kraut N, Peters JM (2007). The small-molecule inhibitor BI 2536 reveals novel insights into mitotic roles of polo-like kinase 1. Curr Biol 17, 304–315.
Liu C, Li Y, Semenov M, Han C, Baeg GH, Tan Y, Zhang Z, Lin X, He X (2002). Control of beta-catenin phosphorylation/degradation by a dual-kinase mechanism. Cell 108, 837–847.
Logan CY, Nusse R (2004). The Wnt signaling pathway in development and disease. Annu Rev Cell Dev Biol 20, 781–810.
Louie RK, Bahmanyar S, Siemers KA, Votin V, Chang P, Stearns T, Nelson WJ, Barth AI (2004). Adenomatous polyposis coli and EB1 localize in close proximity of the mother centriole and EB1 is a functional component of centrosomes. J Cell Sci 117, 1117–1128.
MacLaine NJ, Oster B, Bundgaard B, Fraser JA, Buckner C, Lazo PA, Meek DW, Hollsberg P, Hupp TR (2008). A central role for CK1 in catalyzing phosphorylation of the p53 transactivation domain at serine 20 after HHV-6B viral infection. J Biol Chem 283, 28563–28573.
Mardin BR, Agircan FG, Lange C, Schiebel E (2011). Plk1 controls the Nek2A-PP1gamma antagonism in centrosome disjunction. Curr Biol 21, 1145–1151.
Mardin BR, Lange C, Baxter JE, Hardy T, Scholz SR, Fry AM, Schiebel E (2010). Components of the Hippo pathway cooperate with Nek2 kinase to regulate centrosome disjunction. Nat Cell Biol 12, 1166–1176.
Meijer L *et al.* (2003). GSK-3-selective inhibitors derived from Tyrian purple indirubins. Chem Biol 10, 1255–1266.
Merle P *et al.* (2005). Oncogenic role of the frizzled-7/beta-catenin pathway in hepatocellular carcinoma. J Hepatol 43, 854–862.
Morin PJ, Sparks AB, Korinek V, Barker N, Clevers H, Vogelstein B, Kinzler KW (1997). Activation of beta-catenin-Tcf signaling in colon cancer by mutations in beta-catenin or APC. Science 275, 1787–1790.
Nathke IS, Hinck L, Swedlow JR, Papkoff J, Nelson WJ (1994). Defining interactions and distributions of cadherin and catenin complexes in polarized epithelial cells. J Cell Biol 125, 1341–1352.
Nelson WJ, Nusse R (2004). Convergence of Wnt, beta-catenin, and cadherin pathways. Science 303, 1483–1487.
Ohta T, Xiong Y (2001). Phosphorylation- and Skp1-independent in vitro ubiquitination of E2F1 by multiple ROC-cullin ligases. Cancer Res 61, 1347–1353.
Orford K, Crockett C, Jensen JP, Weissman AM, Byers SW (1997). Serine phosphorylation-regulated ubiquitination and degradation of beta-catenin. J Biol Chem 272, 24735–24738.
Piedra J, Martinez D, Castano J, Miravet S, Dunach M, de Herreros AG (2001). Regulation of beta-catenin structure and activity by tyrosine phosphorylation. J Biol Chem 276, 20436–20443.
Piedra J, Miravet S, Castano J, Palmer HG, Heisterkamp N, Garcia de Herreros A, Dunach M (2003). p120 catenin-associated Fer and Fyn tyrosine kinases regulate beta-catenin Tyr-142 phosphorylation and beta-catenin-alpha-catenin Interaction. Mol Cell Biol 23, 2287–2297.
Quarmby LM, Mahjoub MR (2005). Caught Nek-ing: cilia and centrioles. J Cell Sci 118, 5161–5169.
Roura S, Miravet S, Piedra J, Garcia de Herreros A, Dunach M (1999). Regulation of E-cadherin/catenin association by tyrosine phosphorylation. J Biol Chem 274, 36734–36740.
Steegmaier M *et al.* (2007). BI 2536, a potent and selective inhibitor of polo-like kinase 1, inhibits tumor growth in vivo. Curr Biol 17, 316–322.
Thotala DK, Hallahan DE, Yazlovitskaya EM (2008). Inhibition of glycogen synthase kinase 3 beta attenuates neurocognitive dysfunction resulting from cranial irradiation. Cancer Res 68, 5859–5868.
Vassilev LT, Tovar C, Chen S, Knezevic D, Zhao X, Sun H, Heimbrook DC, Chen L (2006). Selective small-molecule inhibitor reveals critical mitotic functions of human CDK1. Proc Natl Acad Sci USA 103, 10660–10665.
Wang G, Chen Q, Zhang X, Zhang B, Zhuo X, Liu J, Jiang Q, Zhang C (2013). PCM1 recruits Plk1 to pericentriolar matrix to promote primary cilia disassembly before mitotic entry. J Cell Sci 126, 1355–1365.
Weis WI, Nelson WJ (2006). Re-solving the cadherin-catenin-actin conundrum. J Biol Chem 281, 35593–35597.
White MC, Quarmby LM (2008). The NIMA-family kinase, Nek1 affects the stability of centrosomes and ciliogenesis. BMC Cell Biol 9, 29.
Wu G, Xu G, Schulman BA, Jeffrey PD, Harper JW, Pavletich NP (2003). Structure of a beta-TrCP1-Skp1-beta-catenin complex: destruction motif binding and lysine specificity of the SCF(beta-TrCP1) ubiquitin ligase. Mol Cell 11, 1445–1456.
Zhang F, Phiel CJ, Spece L, Gurvich N, Klein PS (2003). Inhibitory phosphorylation of glycogen synthase kinase-3 (GSK-3) in response to lithium. Evidence for autoregulation of GSK-3. J Biol Chem 278, 33067–33077.